C

243128

JPRS-JST-88-003
12 APRIL 1988

FOREIGN
BROADCAST
INFORMATION
SERVICE

JPRS Report

Science & Technology

Japan

JPRS-JST-88-003
12 APRIL 1988

SCIENCE & TECHNOLOGY

JAPAN

CONTENTS

/12223

Development of Optical Isolator Materials, Applications

43067512a Tokyo KINO ZAIRYO in Japanese Oct 87 pp 13-20

[Article by Katsumi Machida, chief; Kazuhiro Nakajima, and Haruo Ishikawa, Electronic Material Laboratories of Sumitomo Metal Mining Co.: "Development and Applications of Optical Isolator Materials"]

[Text] Compact, low-priced, highly reliable optical isolators to be used to cut off the light rays reflected back to the light sources of optical communication or optical measurement systems are in demand today. Sumitomo Metal Mining Co. has developed magnetic garnet thick films as materials for Faraday rotors, which are the main components of optical isolators, using the liquid-phase epitaxial growth method. This paper generally describes the development and applications of the developed materials.

1. Introduction

Optical fiber communications made using laser diodes (LDs) with 1.3- and 1.55-μm wavelengths enable larger amounts of data to be transmitted more accurately at higher speed with less power loss than the conventional telecommunications. However, the LDs used as light sources for optical fiber communications are susceptible to rays reflected from optical fiber junctions and various optical circuit elements; that is, reflected rays entering LDs cause the oscillations of the LDs to be destabilized. LDs whose performance has been improved and which can be coupled with optical fibers with higher coupling efficiency than before are now available. In addition there is growing demand for high-speed digital transmissions to be made by the use of single-mode fibers as well as for analog transmissions to be made by the direct intensity modulation method. Therefore, suppressing the phenomenon caused by reflected light rays as mentioned above is an essential target to be achieved. Such a target can be achieved by inserting an optical isolator between the LD used as a light source and the optical fiber with which the LD is connected.

From the viewpoint of making optical isolators smaller and more stable in performance, the Faraday rotors--main components of optical isolators--are required to meet the following requirements:

1) Their Faraday rotation factors (deg/cm) are small.

2) The variations (deg/degrees C) with temperature of their Faraday's rotation angles are small.

3) Their absorption loss in the oscillation range of LDs are small.

4) The magnetic field strength required for them to achieve magnetic saturation is small.

Faraday rotors for use in the near infrared region used to be made of $Y_3Fe_5O_{12}$ (YIG) produced by the flux method or FZ method. However, YIG has disadvantages such as (1) its Faraday rotation factor is as small as 220 deg/cm at a wavelength of 1.3 μm, (2) it requires as large a magnetic field strength as 2KOe to reach magnetic saturation, (3) with its extinction ratio generally ranging around 35 dB, a high isolation level is difficult to achieve with it, and (4) growing a large crystal of YIG is difficult and takes many hours. At present, Bi [bismuth]-substituted garnet crystal produced by the liquid phase epitaxial (LPE) method is drawing attention as a Faraday rotor material.[1] Substituting Bi for the rare-earth elements contained in magnetic garnet greatly increases the Faraday rotation factor of the garnet without affecting its absorption coefficient. This phenomenon was discovered in 1974 with Bi-added rare earth iron garnet and attracted attention at that time.[2] Recently, studies of the phenomenon have become active again as the garnet has come to be regarded as an optoelectronic material. Growing quality single-crystal garnet containing a large amount of Bi obtained through substitution had been extremely difficult, but the LPE method has made such crystal growing practical.[1,3]

The technique for garnet film formation by the LPE method was originally developed for magnetic bubble memory production. It enables a quality single-crystal film of, for example, $(YLuCaBi)_3(FeGe)_5O_{12}$ with a thickness of about 1 micron to be formed on a $Gd_3Ga_5O_{12}$ (GGG) substrate. The magnetic characteristic of the film can be controlled by adjusting the garnet composition. Furthermore, with quality substrates which measure as large as 3 to 4 inches in diameter being obtainable, a single-crystal film can be formed over an equally large area. The single-crystal film growing technique today enables quality single-crystal film of Bi-substituted garnet with a thickness of 600 μm or more to be obtained as an optical isolator material.[4]

The LPE film for optical isolator was initially proposed for use in horizontal incidence mode. That is, it was first proposed growing Gd:YIG film as an intrasurface magnetic film over a GGG substrate by the LPE method so that rays parallel to the film surface might enter the

film via its end faces. Because the film for use in horizontal incidence mode involves many difficult problems with regard to device designing, vertical incidence-type films which permit vertical incidence of a light beam with a large sectional diameter subsequently came to supersede the former type.[1] What made the idea of using films in vertical incidence mode practical was the development of films containing a large amount of Bi acquired by substitution. The direction in which rays advance in a Bi-substituted film after entering it at right angles is identical with the direction in which the film was grown, so that double refraction is reduced in the film used in vertical incidence mode. To enable substitution of a large amount of Bi, substrates of Ca, Mg, Zr: GGG (a = 12.498 Å) with a large lattice constant are used. It was reported that high-performance material whose insertion loss is 0.2 dB at a wavelength of 1.3 μm and isolation level is 43 dB and which can reach magnetic saturation with a 200 Oe magnetic field had been obtained by forming a film of $(GdBi)_3(FeAlGa)_5O_{12}$ (abbreviated to GBIG) over the above-mentioned substrate.[4]

A feature of the material is that it enables the fabrication of an optical isolator with a small magnet, since the magnetic field strength required by it to reach magnetic saturation is as small as about one tenth of that needed by YIG. A disadvantage of the material is that its Faraday's rotation angle varies greatly with temperature in the isolator operating temperature range (-20 to +60 degrees C), making it difficult to maintain high isolator performance. However, research work on the material aimed mainly at improving its temperature characteristic has been promoted and it is now possible to grow high-performance thick film as optical isolator material good enough for practical use. The material is already in use, particularly, in the near infrared region and the range of its applications is about to expand.

2. Growth of Faraday Rotor Material

2.1 LPE Method

A furnace for growing film by the LPE method is schematically shown in Figure 1. The components of garnet and a flux (PbO, B_2O_3, Bi_2O_3) are put in the platinum crucible, are melted at a temperature of about 1000 degrees C, and are mixed for several hours for homogenization. The melt is then supercooled to below its saturation temperature. Over the surface of the supercooled melt, a GGG substrate is horizontally rotated at 100 r.p.m. with its bottom side dipped in the melt to grow film at a constant temperature in several hours. During the film growing process, the melt temperature is controlled with an accuracy of ±1 degree C in the range of 800 to 900 degrees C and film is grown at a rate of 0.8 to 1 μm/min. As being discussed later, the substrate and garnet differ largely in thermal expansion, so that the film requires gradual cooling.

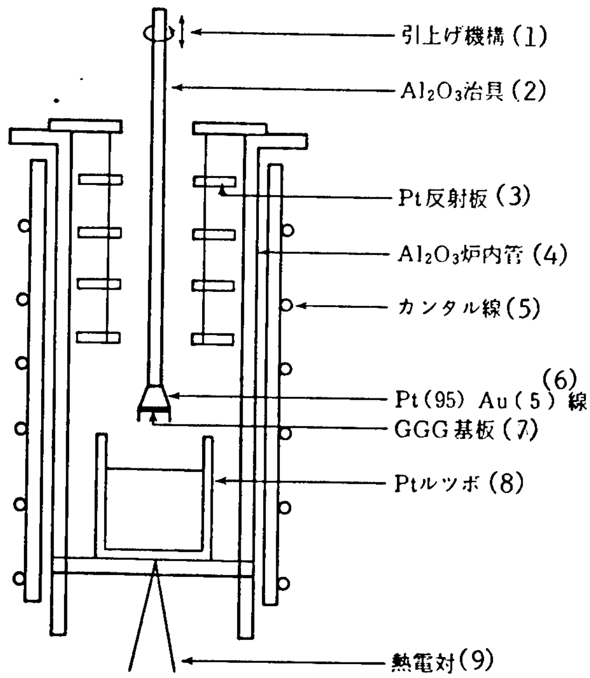

Figure 1. System for Crystal Growing by LPE Method (Sectional View)

Key:

1. Pulling mechanism
2. Al_2O_3 jig
3. Pt reflector
4. Al_2O_3 furnace inner cylinder
5. Kanthal line
6. Pt(95) Au(5) wire
7. GGG substrate
8. Pt crucible
9. Thermocouple

Garnet thick films grown in the early days had many pits. Noting that such pits include hexagonal ones formed to depths of about 50 μm, we analyzed (1) circular pits (measuring up to 5 μm in diameter and 0.1 μm in depth) formed on GGG substrate surface and (2) triangular pits formed in thin film with a thickness of 5 μm, in order to study how they are created and how their shapes change. As a result, we have learned that the circular pits (1) formed on substrate surface grow larger as the film thickness increases, that, in the course of expanding, the plane growth begins to turn into triangular or hexagonal pits, and that the triangular pits (2) grow larger very fast to eventually turn also into large hexagonal pits. Analysis of the central parts of pits formed in film with a thickness of several μm led us to consider that the sources of pits are platinum nuclei. Consequently, it has been known that, in

growing garnet film with a thickness of 200 μm or more, the formation of large pits can be prevented by taking the following steps:[5]

(1) Using quality crystal substrates;

(2) Suppressing the number of platinum nuclei in the melt or in the surface portion of the melt.

When thick film is grown by the LPE method, camber and cracking, which are considered attributable to the difference in lattice constant between the substrate and film at the film growing temperature, are observed to take place. It has been reported that the thermal expansion ($(a_T - a_0)/a_0$; where a_T and a_0 represent lattice constants at temperature T and at room temperature, respectively) of the film and substrate change with temperature as shown in Figure 2.[5] The figure indicates that, at the film growing temperature (about 800 degrees C), there is a thermal expansion difference of 1.5 x 10 between the substrate and the film. That is, even if film is grown such that its lattice constant matches that of the substrate at room temperature, its lattice constant becomes about 0.1 percent larger than that of the substrate when the film is grown. This suggests that, when a film is grown over a substrate, the substrate is caused to camber. We observed the phenomenon by directing a He-Ne laser beam onto a crystal being grown and measured changes in the radius of its curvature.[5] In Figure 3, the solid line represents values calculated using Timoshenko's bimetal model,[6] whereas black dots represent measured values. The figure indicates that the two-layer material comprising a substrate and the film being grown is cambered during the film growing process and that the camber conforms to the bimetal model.

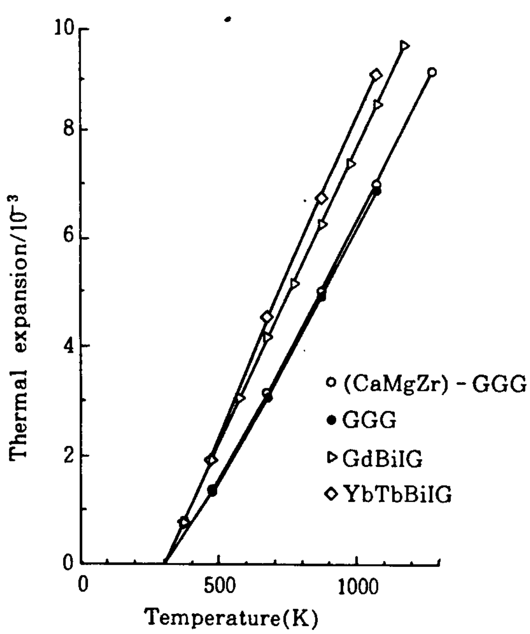

Figure 2. Thermal Expansion Versus Temperature

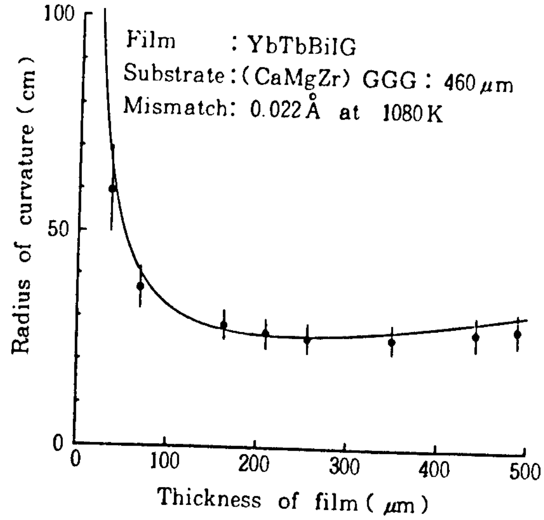

Figure 3. Film Thickness Versus Radius of Curvature

Even if film is grown at a temperature at which its lattice constant matches that of the substrate while it is thin, the substrate eventually became coated with a thick film cambers even after it is cooled to room temperature. We have found that a thick film which does not camber at room temperature can be obtained by growing film under such conditions that the value of its Δa becomes 1.5 to 3.0 x 10^{-3} Å ($\Delta a = a_s - a_f$; where a_s and a_f represent the lattice constants of the substrate and film at room temperature, respectively) while it is thin. Growing a thick film in a state where $\Delta a = 0$ results in obtaining a film cambered to the substrate side. Optimizing film growth by taking into the foregoing into account makes it possible to obtain a camberless thick film of quality crystal. Generally, garnet film is grown only over one side of substrate as a result of taking into account the problem of cambering during the growing process. For garnet film growing on a quantity basis, however, it becomes necessary to form film over both sides of substrate by the LPE method using multistage jigs.

2.2 Temperature Characteristic Improvement

When garnet film is grown by the LPE method, it is necessary to align the lattice constants of the substrate and the film so that a large Faraday rotation factor (θf) may be obtained. When a large number of R ions of c site in the garnet structure are substituted for by Bi ions having a large ion radius, Fe ions of a and d sites may be substituted for by Al and Ga ions whose ion radii are smaller than those of Fe ions. It has been found that, while such a phenomenon of ion substitution leads to an increase in the value of θf, it also causes the temperature characteristics of θf to deteriorate due to a decline in Curie temperature (Tc). For RIG for which Bi substitution is not made, it has been proposed[7] that a composite solid solution consisting of R ions

having temperature coefficients represented by different symbols be used as a means of improving the temperature characteristics of θf. Where a large number of Bi ions are substituted, however, θf is greatly affected by Bi ions and it is difficult to utilize the effect of R ions themselves. In such a case, it is more desirable to try to improve the temperature characteristic of θf by reducing the magnitude of substitution of nonmagnetic ions for Fe ions and thereby causing Tc to rise. Besides serving to increase the value of θf, substitution of a large amount of Bi is also expected to result in causing the temperature characteristic of θf to be improved due to the rise in Tc by the effect of Bi.

In an attempt to find a way of improving the temperature characteristic of θf in growing a thick film of garnet, we experimented in maintaining Bi substitution at a high level and totally preventing Fe ions from being substituted for by nonmagnetic ions during garnet thick-film growing, by means of using (1) R ions with a small radius and (2) substrates with a large lattice constant. In the experiment, the temperature characteristic of θf and Curie temperature Tc of RBiIG film were measured. The results are shown in Table 1 and Figure 4. The θf temperature coefficients indicated in them are for a θf of 45 degrees at room temperature. When the material composition involved is one in which Fe ions are not substituted for by other ions, the lattice constant of the substrate remains unchanged. In such a case, the radius of R ions affects the magnitude of Bi substitution and hence Tc because a great magnitude of Bi substitution enhances superexchange interaction. This effect has been explained as being attributable to the structural as well as electronic contribution of Bi ions which have a large radius and whose spin-orbit coupling constant is large. The increase in magnetic coupling energy attributable to superexchange interaction causes Tc to rise and the θf temperature coefficient to be greatly improved.[4),8)]

Table 1. Curie Temperatures and Faraday Rotation Temperature Coefficients of RIG's

R	Lu	Yb	Tm	Er	Dy	Gd	Y
X	0.80	0.77	0.58	0.30	1.07	0.40	1.31
Tc (K)	583	581	580	574	603	585	611
θf temperature coefficient (10^{-2} deg/K)	7.7	7.7	7.9	8.4	6.2	7.6	5.8
Magnetic field (Oe) needed for saturation	3000	2500	1600	1200	1000	300	1900

$R_{3-x}Bi_xFe_5O_{12}$ $\lambda = 1.3\ \mu m$

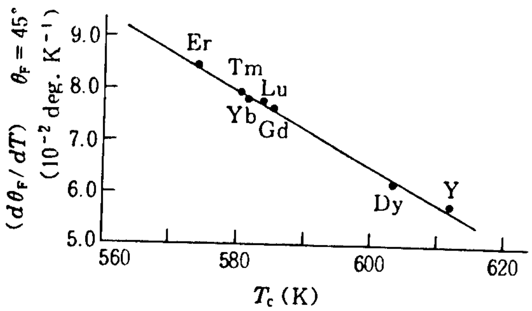

Figure 4. Curie Temperature vs. Temperature Coefficient

For example, when Dy or Y is used as R ions, a temperature coefficient equivalent to that, 0.05 deg/degrees C, of bulk YIG can be obtained. Moreover, as shown in Figure 5, the values of θf stand at 1500 and 2300 deg/cm for them, respectively, indicating that they offer very high performance compared with YIG. However, in the case of YBiIG, it requires a strong magnetic field to reach magnetic saturation as shown in Table 1; whereas, in the case of DyBiIG, an absorption band peculiar to Dy exists on the 1.3-μm band. After giving consideration to these conditions, we came up with an idea of combining rare-earth elements.

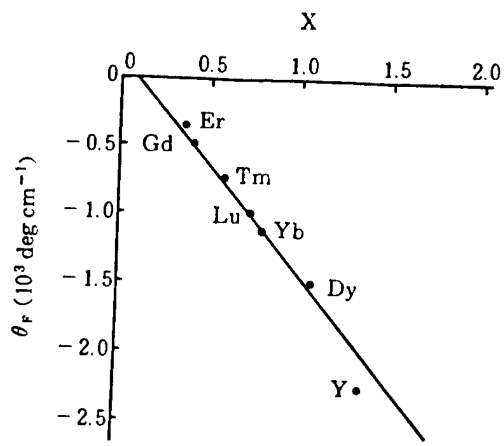

Figure 5. Bi Concentration in $R_{3-x}BiXFe_5O_{12}$ versus Faraday's Rotation Angle at 1.3 μm Wavelength

As a new composition, we have selected a rare-earth combination of YB + TB for the following reasons: (1) Yb having a small ion radius permits substitution of a large amount of Bi, (2) Tb iron garnet can reach magnetic saturation with a small magnetic field, and (3) neither

Yb iron garnet nor Tb iron garnet has an absorption band on the 1.3-1.55 μm band. We experimented in thick film growing with Yb and Tb mixed at varied ratios. A melt composition ratio between Yb and Tb of 1:3.65 resulted in growing of quality-crystal thick film with superior characteristics.[4] In Table 2, the magneto-optic characteristics at 1.3- and 1.55-μm wavelengths of GBIG and YbTbBiIG at room temperature are compared. The isolation and insertion loss values given in the table were obtained by making measurements on samples coated for reflection prevention. The values of θf measured on YbTbBiIG are larger than those measured on GBIG. YbTbBiIG excels GBIG in terms of temperature coefficient particularly in the long-wavelength region. As the curves of θf value dispersion by temperature shown in Figure 6 indicate, the value of θf decreases with lengthening wavelength; so that the film thickness needed to enable the polarized wave plane to rotate through 45 degrees increases as the wavelength enlarges. Faraday rotor samples 15 mm square and 3 mm square are shown in Photo 1 [omitted].

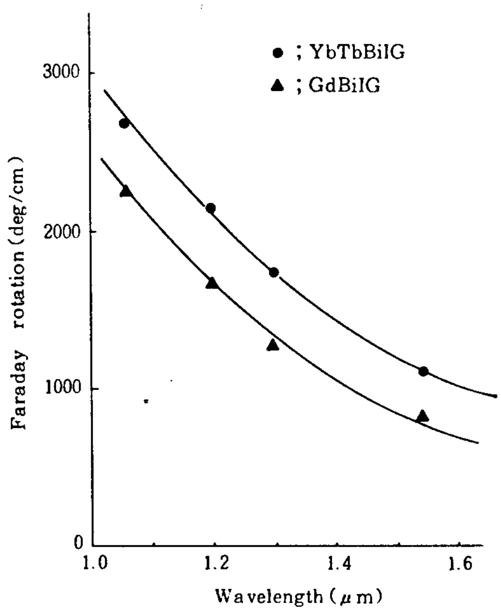

Figure 6. Faraday's Rotation Factor Dispersion by Wavelength

The causes of variation of θf with temperature include first the foregoing factors attributable to the materials themselves and second the variation with temperature of oscillation wavelength of the LD used as light source. The oscillation wavelength of an LD shifts toward the long-wavelength region with increasing temperature. There are cases in which a temperature rise from 0 degrees C to 60 degrees C causes the oscillation wavelength of 1.3 μm of an LD to be shifted by about 80 nm. Such a temperature-susceptibility of LDs poses a problem particularly

Table 2. Magneto-Optic Characteristics of Faraday Rotor Materials

Characteristic Items	Values			
Sample	$(GdBi)_3\ (FeAlGa)_5O_{12}$		$(YbTbBi)_3Fe_5O_{12}$	
Substrate	$(GdCa)_3\ (GaMgZr)_5O_{12}$		$(GdCa)_3\ (GaMgZr)_5O_{12}$	
Wavelength (μm)	1.3	1.55	1.3	1.55
Faraday's rotation factor (deg/cm)	1300	900	-1800	-1200
Temperature coefficient of Faraday's rotation angle (deg/degrees C)	-0.11	-0.16	0.06	0.07
Film thickness (θF = 45 degrees) (μm)	350	500	250	375
Insertion loss (dB)	0.2	0.4	0.4	0.3
Isolation (dB) (backward loss/forward loss)	43	34	38	40
Magnetic field strength required for saturation (Oe)	$\sim$200		$\sim$1000	

when an isolator is to be used in combination with an LD. We have found a way of putting together materials whose θf temperature coefficients are represented by different symbols to obtain a composite material with a desired temperature coefficient.[9] Assume there are two materials A and B whose θf values (deg/cm) are represented by θFa and θFb, whose thicknesses (μm) are represented by la and lb, and whose f temperature coefficients are represented by $d\theta Fa/dT$ and $d\theta Fb/dT$, respectively. When the two materials are to be used to produce a composite optical-isolator material, they are required to meet the following condition:

$$| l_a \cdot \theta F_a + l_b \cdot \theta F_b | = 45° \cdots\cdots\cdots\cdots \quad (1)$$

The corresponding temperature coefficient r is expressed as:

$$r = l_a \cdot d\theta F_a / dT + l_b \cdot d\theta F_b / dT \cdots\cdots \quad (2)$$

As far as the temperature range in which the values of $d\theta Fa/dT$ and $d\theta Fb/dT$ stay constant is concerned, the temperature coefficient of either the Faraday rotor or the combination of the Faraday rotor and LD can be made 0. As materials A and B having different θf temperature coefficients, we selected A:GBIG and B:YbTbBiIG. Faraday's rotation angles of A and B are 55.2 deg. and -99.4 deg. (T = 30 degrees C), respectively, at a wavelength of 1.3 μm. The variations with temperature of θf values of materials A and B as well as the combination of the two materials are shown in Figure 7. Table 3 lists characteristics of the two materials A and B. By combining the two materials, we have succeeded in obtaining a composite material with as low a temperature coefficient as 2 x 10 deg/degrees C. It has high potential as an isolator material for use where the temperature coefficient of the material to be used bears particular significance.

Table 3. Characteristics of Two Types of Garnet Film

特性(2) ＼ (1)材料	A	B
膜 厚(3) (μm)	428	515
θ_f (deg/cm)	1289	−1931
$d\theta_f/dT$ (deg/cm·°C)	−3.29	2.77

A : $(GdBi)_3 (FeAlGa)_5 O_{12}$
B : $(YbTbBi)_3 Fe_5 O_{12}$.

Key:

1. Sample
2. Characteristics
3. Film thickness

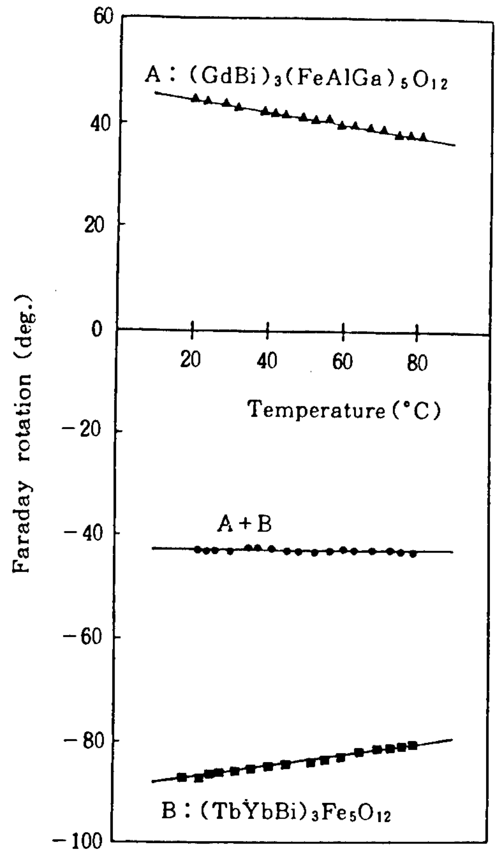

Figure 7. Variation of Faraday's Rotation Angle with Temperature

3. Test Manufacture of Optical Isolators

We test-manufactured 1.3-μm wavelength optical isolators using YbTbBiIG and GBIG. Their structure is schematically shown in Figure 8. The polarizer comprises a polarized beam splitter (PBS) and the magnet is a doughnut-shaped Sm-Co plastic magnet measuring 10 mm in outer diameter, 3 mm in inner diameter, and 1.5 mm in thickness. Every optical component has been coated to prevent 1.3-μm wavelength reflection. Each PBS is attached with a magnetic holder which is held in position by the magnet. The PBS held in position in that way can be turned with ease so that adjustment of the polarized wave plane is facilitated. The values of insertion loss and isolation level measured on the two materials as well as on the two isolator modules containing Faraday rotors made of the two materials are listed in Table 4. An optical isolator of the same structure containing more compact polarizers, measuring about 5 mmø by 5 mm each, made of rutile or calcite can be directly coupled with a laser diode. Figure 9 shows the setup of a fiber-to-fiber type optical isolator we fabricated. In the isolator, the light coming out of each fiber is led through a rod lens (0.25p) for conversion into parallel

rays. A pair of PBS's and a Faraday rotor (GBIG) are located between the two rod lenses. We aligned GI50 fibers with the isolator using two electric manipulators (manipulatable in 0.1-μm steps). An isolation level of 36 dB and an insertion loss of 1.5 dB were measured on the setup.[10]

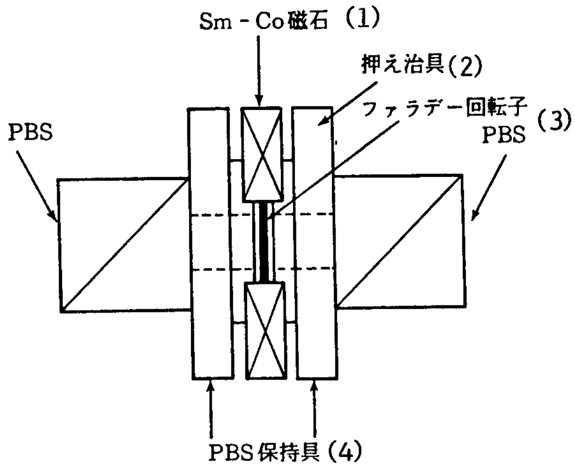

Figure 8. Optical Isolator Structure

Key:

1. Sm-Co magnet
2. Holding jig
3. Faraday rotor
4. PBS holder

Table 4. Characteristics of Optical Isolator Modules

	Film	Module
BdBiIG:		
Insertion loss	0.6 dB	0.9 dB
Isolation	36 dB	36 dB
YbTbBiIG:		
Insertion loss	0.7 dB	1.0 dB
Isolation	36 dB	36 dB

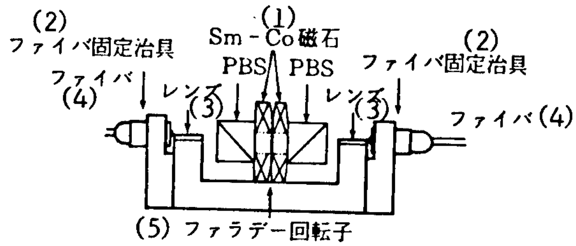

Figure 9. Fiber-to-Fiber Type Optical Isolator Setup

Key:

1. Sm-Co magnet
2. Fiber fixing jig
3. Lens
4. Fiber
5. Faraday rotor

4. Application to Magnetic Field Sensors

Bi-substituted garnet film with its great magneto-optic effect has been collecting attention from the viewpoint of application to magnetic field sensors, too. Much expectation is placed on it as a highly sensitive material whose properties are not very temperature-susceptible and which enables parts size reduction. Figure 10 shows the theory of magnetic field sensor operation. A magnetic field sensor system includes a Faraday rotor. A polarizer is placed on one side of the Faraday rotor and analyzer on the other side. They are set in a 45 degree-rotated position relative to each other so as to maximize the change in the quantity of light caused when the place of polarization is rotated by the Faraday rotor. The change in the quantity of light caused when the Faraday rotor tilts the plane of polarization by $\pm\theta$ is given as ($\pm\sin 2\theta = \pm\sin(2V_E \cdot Hex)$); where V_E represents an effective Verdet's constant and Hex represents an external magnetic field. For magnetic garnet, V_E is defined as ($V_E \doteqdot \theta f/Hs$), and Hs is defined as the magnetic field needed to achieve magnetic saturation. The requirements of magnetic-field sensor material include that its Verdet's constant is (1) large, (2) unaffected by temperature changes, and (3) unaffected by changes in magnetic field strength. YIG consisting of rare-earth iron garnet crystal has an optical wavelength of 1.3μm and a V_E value of 0.26 deg/Oe · cm which are far greater than those of lead glass.[11] Furthermore, the value of θf of Bi-substituted rare-earth iron garnet is larger than that of YIG by one order of magnitude or more; so that it is possible to obtain a correspondingly larger V_E value for Bi-substituted rare-earth iron garnet by adopting rare-earth elements whose saturation magnetization is small. Figure 11 shows the V_E dispersion by wavelength of GBIG and YbTbBiIG. Their V_E values at varying wavelength shown in the figure are very large compared with those of YIG. Figure 12 shows the hysteresis curve of magnetization of a GBIG sample measuring 5 by 5 by 0.2 (t) mm. It indicates that the magnitude of Faraday's rotation

angle is proportional to that of magnetization and that, because of the relationship between the magnitude of magnetization and the strength of external magnetic field, Faraday's rotation angle linearly changes with the strength of external magnetic field.

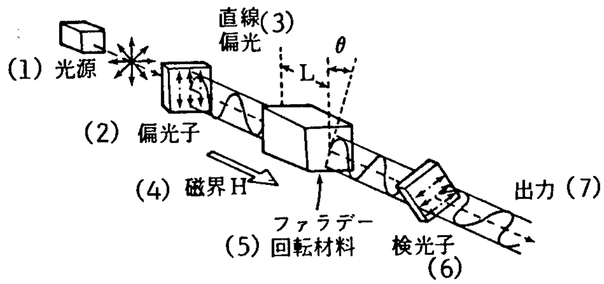

Figure 10. Theory of Magnetic Field Sensor

Key:

1. Light source
2. Polarizer
3. Linearly polarized light
4. Magnetic field H
5. Faraday rotor material
6. Analyzer
7. Output

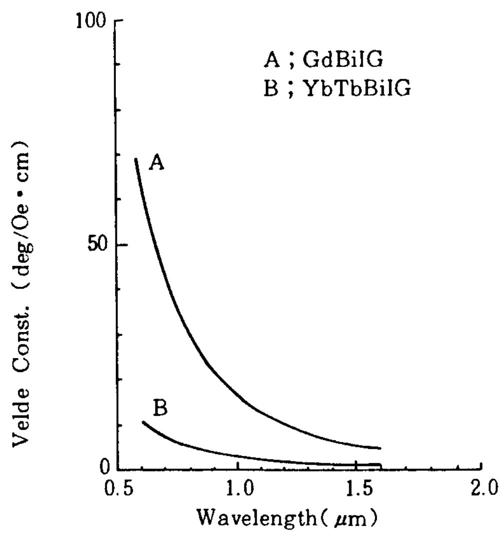

Figure 11. Dispersion of Effective Velde Constant According to Wavelength

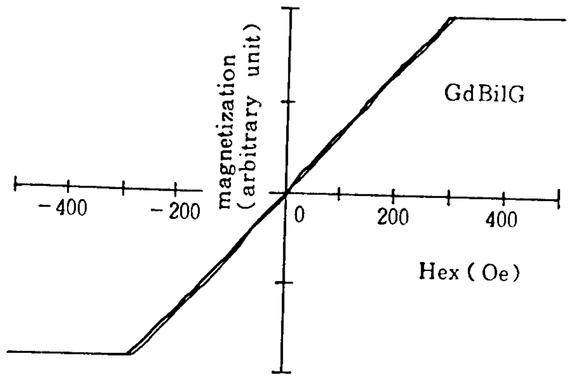

Figure 12. Magnetization Curves

5. Conclusion

A technique which enables generally superior Faraday-rotor materials to be produced by the LPE method has been described. Magneto-optic applications constitute an area where Japan is advanced in R&D. The process for growing thick films of garnet by the LPE method is unique to Japan. Besides being usable in optical switches and optical circulators as discussed in the foregoing, magnetic garnet film can also be used in devices such as optical modulators. It is hoped that research work for developing more applications of magnetic garnet films progress more and more from now on.

BIBLIOGRAPHY

1. T. Hibiya, Material for 38th study meeting of Applied Magnetism Society of Japan [Nihon Oyo Jiki Gakkai], 38-29 (1985).

2. K. Shinagawa and T. Taniguchi, "Jpn. J. Appl. Phys." 13, 1664 (1974).

3. P. Hansen and J. P. Krumme, "Thin Solid Films" 114, 69 (1984).

4. K. Machida et al., "J. Appl. Phys." 61, 3256 (1987).

5. K. Machida and Y. Asahara, ISMO'87 Kyoto April (1987).

6. S. Timoshenko, "J. Opt. Soc. Am." 11, 233 (1925).

7. S. Matsumoto, 1984 Shingaku So Zentai, 1005 (1984).

8. K. Nakajima, SHINGAKURON (c), J.70-C1 120 (1987).

9. Y. Asahara, et al., Proceedings of 10th lecture meeting of Applied Magnetism Society of Japan, 4aE-1 (1986).

10. H. Ishikawa, et al., 4th Optical Fiber Sensor Workshop, WOFS4-11 (1987).

11. T. Taniguchi, et al., NATIONAL TECHNICAL REPORT 29, 716 (1983).

20109/09599

Design of Functionally Gradient Material Examined

43067512b Tokyo KINO ZAIRYO in Japanese Oct 87 pp 31-43

[Article by Masayuki Niino, Aeronautical and Space Technology Research Institute: "Design of Functionally Gradient Material by Complexing Technique"]

[Excerpts] 1. Concept of Complexing Technique

1.1 Background

Ultraheat-resistant material technology is among the fundamental technologies on which whether next-generation space and aeronautical vehicles and fusion reactors can be successfully developed depends, and R&D on ultraheat-resistant materials is being energetically promoted in many fields. With regard to space shuttles and fusion reactors, it is required that R&D be expedited on a nationwide scale. As for the materials for use in such fields, which are expected to be subjected to a very severe ultrahigh-temperature environment, increasingly severe requirements have been incorporated in the targets to be achieved in relevant material development.

Take the development [1] of a space shuttle which is to travel in space at a speed exceeding Mach 25, for example. To make such a space shuttle perfectly reusable, the heat-blocking materials to be used in its nose section or structural materials for its engine are required to withstand a surface temperature of 2000 K and a temperature head of 1000 K. Meeting such requirements are beyond the conventional techniques.

Coating metals or alloys with ceramics is known as a conventional method of making heat-resistant materials also heat-blocking. There are also other methods such as the ion plating method in which protective film is impulsively vacuum-evaporated on base materials, the plasma CVD method in which base materials are coated with heat-blocking film using a vapor-phase synthesis technique, and the ion beam method. However, the conventional material techniques comprising coating or plating techniques are not based on positive measures for thermal-stress

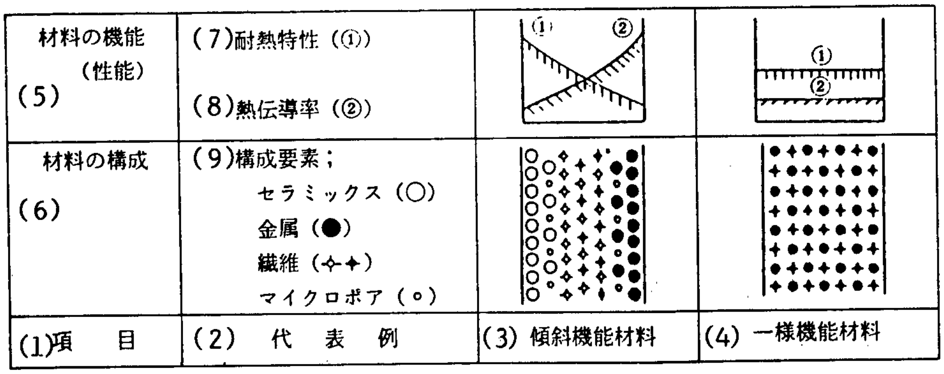

Figure 1. Concepts of Functional Materials

Key:

1. Item
2. Typical examples
3. Functionally gradient material
4. Functionally uniform material
5. Material function (performance)
6. Material composition
7. Heat-resistance characteristics (1)
8. Thermal conductivity (2)
9. Component elements:
   - Ceramic (○)
   - Metal (●)
   - Fiber (✧✦)
   - Micropore (∘)

reduction incorporated in material design. What are done in this regard in the stage of material design are, at the most, attempts to merely change material compositions by degrees. Therefore, the conventional heat-resistant materials pose many problems. They include, for example, exfoliation and fracture, which are attributable to repeated exposures to thermal stress or aged deterioration, and reduction in corrosion resistance due to cracking.

Against such a technical background, a new concept of technical design intended to enable microstructural material elements to be controlled multidimensionally and continuously beginning from the material production stage has been proposed.

1.2 Technical Features

It is impractical to use conventional homogeneous materials as structural members under such a severe condition that the material surface temperature reaches 2000 K. Hence, it is necessary that the structural members to be used in such a severe environment be made of nonhomogeneous materials consisting of more than one element. As shown in Figure 1, the outer surface portion that comes in contact with gas as hot as several thousand degrees of a functional material may consist of heat-resistant ceramic, whereas the low-temperature side that is cooled by liquid hydrogen or liquid metal of the same material may comprise metal having high thermal conductivity and high mechanical strength. That is, it is necessary to make proper function division within the same material consisting of different elements, some usable at high temperature and others suitable for use at low temperatures. In order to synthesize such a nonhomogeneous material, it is essential to acquire a technique which enables a material synthesis process capable of continuously varying the state of metallic or ceramic raw material, for example, from a powdery state to a fibered state or to flakes or droplets based on the results of computerized simulation of ceramic-to-metal intermaterial transition. Such a technique is referred to as a complexing technique. It is a technique for artificially controlling many micro "elements" of a material.

The complexing technique makes it possible to obtain gradient material functions which cannot be realized by the conventional material techniques used to pursue uniform material functions (performance). That is, the new technique enables production of so-called functionally gradient materials. As illustrated in Figure 1, the technique makes it possible to obtain material whose composition, unlike those of the conventional materials having uniform functions, is continuously varied as required to obtain arbitrarily distributed functions.

The complexing-oriented techniques for material production that have been in use include hybrid material and composite material techniques. However, the complexing technique notably differ from such conventional techniques in major aspects such as design concept and material

composition. For example, as outlined in Table 1, whereas the complexing technique comes between the hybrid material technique and composite material technique in terms of texture-controllable region and bond format, it differs totally from the other two in material design concept. The material design concept on which it is based aims at producing materials whose functions are internally distributed to be gradient in a manner convenient for coping with the conditions of the operating environment so that the performance of individual elements of such materials is fully made use of. It is expected that these new and conventional material techniques, though they partly compete with one another, will further be developed in a complementary manner.

2. Expectations for Functionally Gradient Materials

2.1 Thermal-Stress Reducing Effect

The largest problem with nonhomogeneous materials (including laminated materials) which are generally composed of ceramics and metals is the existence of interfaces in them. There are many cases in which the production and use of nonhomogeneous materials are restricted due to great mismatching in thermal expansion and other physical properties at interfaces. More concretely, a thermal transition from high temperature to room temperature which takes place in the process of production of a nonhomogeneous material or a large temperature difference produced between the front and back sides of a nonhomogeneous material when it is put to use causes excessive thermal stress to be generated in the material. In many cases, such excessive thermal stress results in fracturing the material. Thus, how to suppress thermal stress is an important point to be considered in developing ultraheat-resistant nonhomogeneous materials.

The greatest advantage of functionally gradient materials is that the distribution of elements making them up can be continuously varied in such a way that the generation of thermal stress in them can be reduced.

How the thermal stress occurring in functionally gradient materials can be reduced will briefly be explained in the following:

2.1.1 Models of Thermal Stress Caused by Steady-State Thermal Conduction[2)]

For an infinite flat plate having a dimensionless thickness of $0 \leqq X \leqq 1$ as shown in Figure 2, we defined steady-state thermal conduction equations, concentration distribution functions for two components A and B, and physical-property distribution functions. The interior properties of each functionally gradient material are to be determined according to the component mixture average rule. Based on these conditions, we studied functionally gradient materials with varied component concentration distributions, as shown in Figure 3, to probe for the condition of each functionally gradient material that results in

Table 1. Composite-Oriented Material Production Techniques

Item	Hybrid Material Technique	Complexing Technique	Composite Material Technique
Design concept	Composition at molecular or atomic level	Computer utilization for designing according to operating environment and function requirement	Multiplier effects of merits of different materials
Texture control region	1 Å to 0.1 μ	100 Å to 10 mm	0.1 μ to 1 m
Bond format	Intermolecular force	Intermolecular force/chemical bond/physical bond	Chemical bond/physical bond
Texture uniformity			
Micro	Homogeneous/nonhomogeneous	Homogeneous/nonhomogeneous	Nonhomogeneous
Macro	Homogeneous	Nonhomogeneous (Continuous texture distribution)	Homogeneous
Function uniformity	Uniform	Gradient	Uniform

minimizing the magnitude of thermal stress generated in it. As a result, we found that, for each combination of components A and B, there is an optimum distribution of component concentration which results in minimizing thermal stress generation. The optimum component-concentration distribution curve plotted for SiC/C is shown in Figure 4. It was also known that adding a third component with high strength or one which contains micropores and whose Young's modulus is low to a functionally gradient material according to the distribution of thermal stress in the material is also effective in reducing the magnitude of thermal stress occurring in the material. An example of optimum three-component distribution curve is shown in Figure 5.

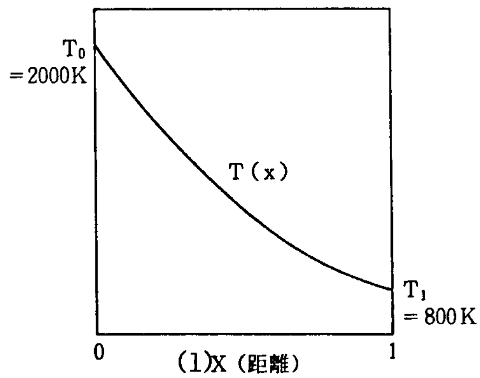

Figure 2. Temperature Distribution on Infinite Flat Plat

Key:
1. X (distance)

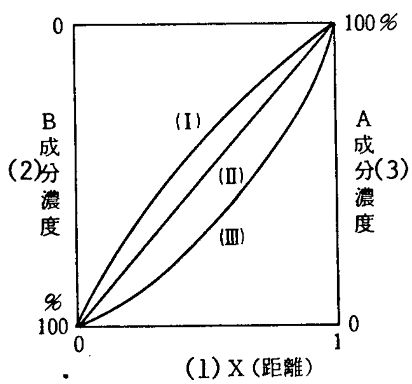

Figure 3. Various Concentration Distribution Functions

Key:
1. X (distance)
2. B-content concentration
3. A-content concentration

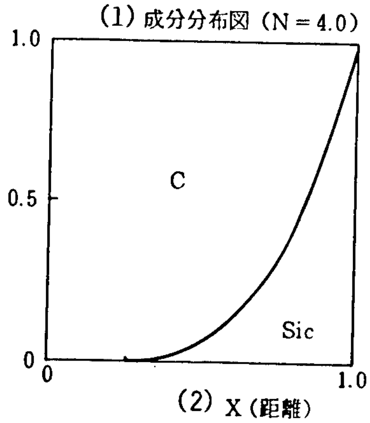

Figure 4. Optimum Composition Distribution of SiC/C

Key:

1. Content distribution diagram
2. X (distance)

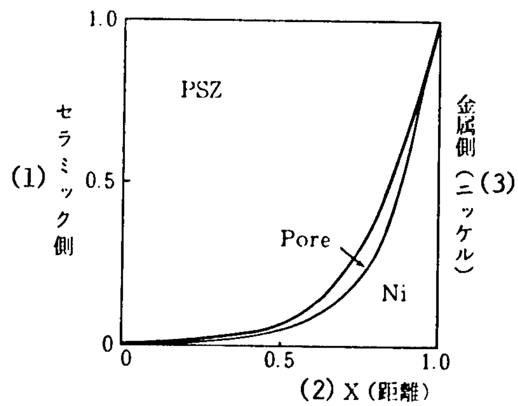

Figure 5. Example of Optimum Three-Component Distribution

Key:

1. Ceramic side
2. X (distance)
3. Metal side (nickel)

Based on the design concept as described in the foregoing, some attempts have been made to produce materials with gradient composition at an R&D level and it has experimentally been ascertained[3),4)] that properly controlling material composition in such a way results in largely reduced thermal stress.

Ultraheat-resistant materials capable of fully functioning in a severe thermal environment where their surface temperature reaches 2000 K and they are subjected to as large a temperature head as 1000 K can be realized only through material design and production based on the concept of functionally gradient material.

2.1.2 Models of Thermal Stress Due to Temperature History Experienced During Production Process

Thermal stress generation is not limited to ultraheat-resistant materials which are subjected to high temperatures. When two materials whose coefficients of thermal expansion are different are joined, thermal stress is generated in the joined material. Even if such materials can be joined at high temperature in the production process, the joint usually develops cracks due to the thermal stress generated when the joined material is cooled to room temperature.

How functionally-gradient materials are effective in solving the problem of thermal stress resulting from material joining will be explained in the following:

Figure 6 shows thermal stress contours calculated[3] for two PSZ/W models, one consisting of W and ZrO_2 directly joined by sintering and the other having a gradient composition. The models analyzed are solids of revolution symmetrical about axis. They have a temperature history of ΔT = 1400 K attributable to the process of cooling from sintering temperature to room temperature. Figure 6 indicates that, even though the number of grades of composition incorporated in the functionally gradient model is only six, the magnitude of thermal stress generated in it is about one sixth of that generated in the directly joined model. In fact, when direct-joint type samples were produced, they developed cracks during the process of cooling to room temperature, whereas samples with a gradient composition recorded a joint strength of 400 Mpa.

Thus, use of the gradient composition control technique or complexing technique makes it possible to join a metal with a ceramic or a ceramic with a different type of ceramic.

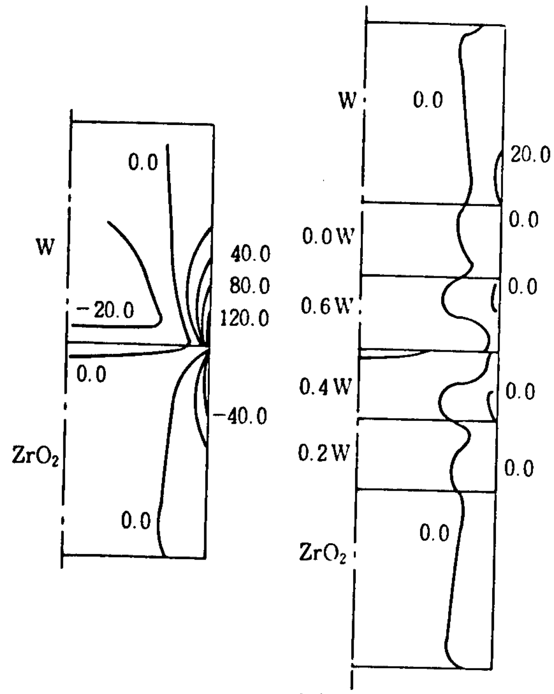

(1) (川崎ら, 文献[3])

Figure 6. σ_z Stress Contour (kg/mm^2)

Key:

1. (Kawasaki, et al.[3])

If a complex body (a minimum structure of functionally gradient material) as shown in Figure 7 can be produced, it becomes possible to produce mechanical components partly comprising ceramics; the metal portion of such a complex body can easily be joined to a different metal part. If such complex parts become producible, the parts of ceramic engines, development of which is being positively promoted, parts of high-temperature devices, or parts required to be wear-resistant or corrosion-resistant of any device can be made of materials consisting of ceramics and metals.

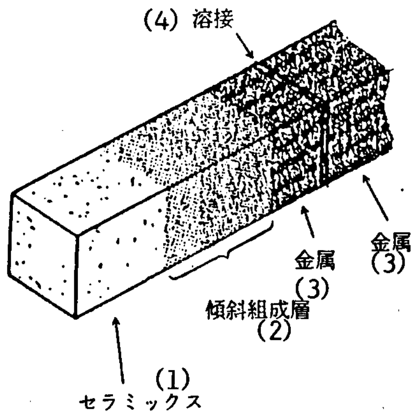

Figure 7. Complex Part Consisting of Ceramic and Metal

Key:

1. Ceramic
2. Section with gradient composition
3. Metal
4. Welding

2.1.3 Pre-Strain Design Models

As widely known, in a means of stress reduction used in producing structural members for buildings, structural members are given pre-strain when they are produced so that the pre-strain counterbalances the strain created in them when they are put to use. It is necessary to positively consider the adoption of such a technique also in designing thermal stress reduced-type materials.[5] Assume that, in a material being used in a temperature state as shown in Figure 8, compressive thermal stress as represented by the curve marked "R" is generated. To prevent the material from being exposed to excessive thermal stress when it is put to use, tensile stress as shown in Figure 9 may be given to it when it is produced so that, when it is put to use, the stress in it will be counterbalanced as shown in Figure 10. Thus, to provide a structural material with such tensile stress beforehand, it is necessary to produce the material in an environment where a temperature difference close to that to which the material is expected to be subjected when it is put to use is present. Simulating such a temperature difference will require many difficult problems to be solved. Nevertheless, it is hoped that research work on the technique for temperature-head simulation will positively be advanced from now on as an important elementary portion of the research work on the design concept for functionally gradient materials aimed at thermal stress reduction.

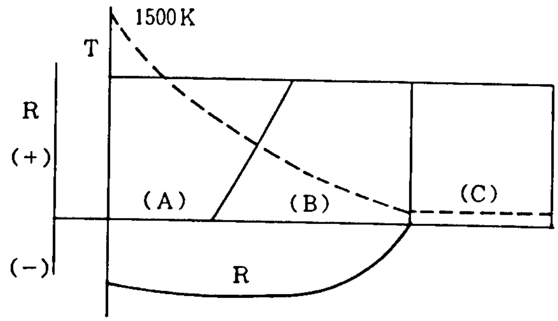

Figure 8. Temperature and Thermal Stress Distributions in Material in Use

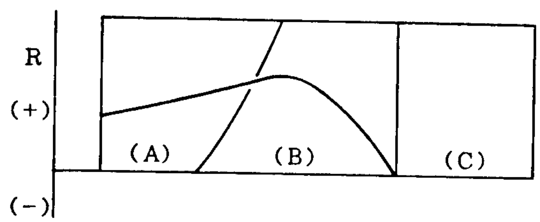

Figure 9. Pre-Strain Stress Distribution

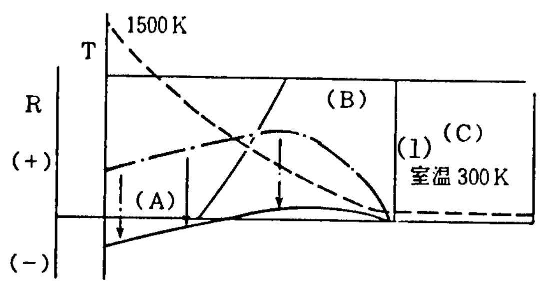

Figure 10. Stress Counterbalancing

Key:

1. Room temperature, 300 K

2.2 Benefits of Functionally Gradient Materials

2.2.1 Functions for Nuclear Applications

Special-purpose materials for use in fusion reactors are among those development of which is strongly required for the promotion of nuclear energy utilization. In nuclear fusion, an ultrahigh-temperature plasma is confined to a vacuum container (blanket) by the force of a magnetic field. The wall surface (first wall) of the container is, as a matter of course, subjected to high temperatures and, moreover, it is radiated with high-energy neutrons generated when fusion reactions take place. The functions required when making nuclear fusion include one for taking out nuclear energy and another for breeding tritium used as nuclear fuel. Before a fusion reactor can be built, many problems have to be solved, even only with regard to heat-conductive flow and structural strength. The materials used in the first wall, tritium breeder and various measuring devices are damaged as they are irradiated with a large quantity of neutrons. It is therefore necessary to develop highly radiation-resistant materials based on the results of fundamental analysis and assessment of such damage to materials. What contribution can functionally gradient materials make toward achieving this target?

When consideration is given to design of the first-wall material, it can be said that the first-wall material must be a layered composite material consisting of stainless metal for structural members and a heat-resistant ceramic. If it has a simple two-layer structure, it will pose problems such as exfoliation due to heat conduction and void formation or gas generation at the interface. As for the ceramic part, it should have plural ceramic layers of different atomic compositions, rather than a single layer, designed by taking into consideration the cross section of nuclear reaction made with neutrons. Besides, it will be necessary for the material to have a structure which physically enables transmission of gases so that gases such as H and He generated by nuclear reactions may be removed. For example, whether the permeable structure of artificial leathers made of organic macromolecules is applicable to the first-wall material should be studied. If the portion of first-wall material surface to which metal is to be bonded is composed of a mixture of metal and ceramic, the detrimental effect of strain due to heat conduction or thermal expansion at the interface in the material will be reduced. It will be possible, for example, to inject fast ions such as Si, C, and O ions from a metal surface to a certain depth and, thereby, form various ceramic microbodies in the metal. When metal is given a ceramic component in such a way, it will be possible to arbitrarily vary the composition of the metal in the direction along its depth. Repeating the process of test-producing various materials using the above-described method, measuring their heat transfer characteristic, heat resistance, and mechanical strength, and assessing their radiation resistance in the foregoing manner will enable increasingly good materials to be developed. Other methods which will be practicable for material development include depositing ceramics on

the heated surface of a metal and forming a composite layer in the metal by thermal diffusion.

Next, let's consider organic composite materials which can be used as superconductive-magnet insulators or as materials for the containers for such insulators. It will be possible to study data on the degradation due to radiation of different materials and the relationship between their degradation and temperature at which they are irradiated; then to design a composite material in which components suitable for use at low temperatures and those suitable for use at high temperatures are layered such that the composite material has a gradient composition optimum as to its functions for thermal or nuclear applications.

It is thought that materials having single compositions or uniform structures cannot be used under the most severe conditions such as those involved in nuclear fusion. To develop materials for use under such conditions, it is necessary to design functionally gradient atomic configurations.

2.2.2 Functions for Medical and Organismic Applications

Artificial teeth, bones, and joints have become available for practical use. What is given serious concern when an object is planted in a human body is the possibility of rejection. Hence, objects to be planted in human bodies are made of materials (e.g., apatite) compatible with human bodies or inert materials (such as alumina, sapphire, stainless steel, and titanium). The real teeth, bones, and joints are light and are appropriately tough and hard. In them, inorganic parts and organic coupling parts are cleverly combined. Particularly, the joints constitute ideal structural materials which are flexible and have functions for self-lubrication and self-repair. They are quite suitable to be a model of complex materials targeted by the present study. Figure 11 shows the structure of an artificial tooth made using the gradient composition control technique. The surface portion of the root artificial tooth to be buried in the gum is made of porous apatite; inner part of the root is less porous. The portion of the tooth that is to project from the gum is covered with a hard ceramic whereas the inner part of that portion is made of a ceramic with high toughness so as to keep the tooth strong enough. When an artificial tooth like this is set in the gum of a human, organismic tissue infiltrates into the porous root of the artificial tooth to securely hold the tooth in position; whereas the ceramic making up its central part augments its mechanical strength.

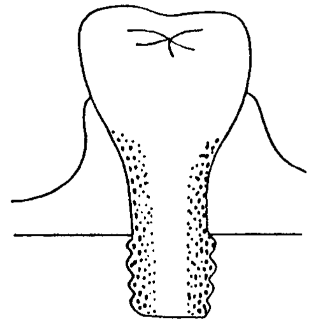

Figure 11. Artificial Dental Root With Gradient Porosity Distribution

It will also be possible to make artificial bones more compatible with living bodies than they are now by adopting a structure comprising an outer and a central part made of porous apatite with an intermediate part made of light, strong material coming in between. As for artificial joints, it may be possible to make them more flexible by adopting a structure which enables them to be joined with cartilage, chords or ligaments or by producing them from a complex material containing organic components.

In the field of artificial internal organs, it is considered that complex bodies made of organic materials can play an important role. Since artificial organs directly affect the patients' lives, their materials are required to have higher performance than those for artificial teeth or bones. They must be compatible with living bodies (rejection, congestion, or thrombi is not allowable), flexible and reliable and must have required functions (e.g., selective permeability required of the material for artificial kidneys). It will be impossible to develop a uniform-structure material which can meet all the requirements. However, it might be possible to synthesize materials which can meet all the requirements by polymerizing various macromolecule materials in a gradient composition. If such materials become producible, further progress will be enabled in the development of artificial hearts and kidneys as well as artificial adjustable crystalline lenses.

Furthermore, it may become possible in the distant future to synthesize proteins and macromolecules having complicatedly distributed compositions in a self-controlled way using gene-handling techniques.

With the longevity of the population increasing, artificial teeth, bones, and organs will be in increasing demand as replacements for degraded real ones. In an era in which man's life span is about 80 years, the technique for gradient composition control is expected to come to play an important role in enabling people to maintain their health through the latter halves of their lives.

2.2.3 Functions for Electric and Magnetic Applications

Electronic apparatuses have been growing smaller and lighter. To keep up with them, electronic parts are also required to be smaller, lighter, and mountable in higher density. Use of the technique for gradient composition control will make it possible to produce electronic parts unified with a substrate or three-dimensional composite electronic parts.

It will also be possible to enhance the performance of individual electronic parts by using the technique in various ways. Possible applications of the technique range so widely that not all of them can be discussed in this paper. Examples of applications constituting only a very limited portion of them will be discussed in the following:

(1) Electro-ceramics

Piezoelectric ceramics such as PZT are used as materials for various electronic parts. Typical ones among such electronic parts include ultrasonic vibrators, ceramic filters, sonars, sensor arrays for ultrasonic diagnostic systems, piezoelectric transformers, piezoelectric actuators, and pyroelectric sensors. For ultrasonic vibrators and ceramic filters, temperature coefficients and spurious emission (resonance and oscillation at other than the target frequency) are factors in causing problems. At present, they are controlled through material composition adjustment. It may be possible to develop such parts with enhanced performance by making their element composition gradient so as to achieve an optimum composition distribution with regard to piezoelectric constant and temperature coefficient.

For sonars or sensors for ultrasonic diagnostic systems, acoustic matching between them and the objects of measurement is a factor in causing problems. Presently, such devices have metal blocks or materials such as plastic and rubber bonded to them for acoustic matching or absorption purposes. However, such a measure does not free them from problems such as failure due to adhesive degradation and spurious emission or S/N ratio deterioration due to acoustic discontinuity. The gradient composition control technique may enable the devices to be improved with regard to the above problems. It may also be possible to develop new piezoelectric materials by applying the technique to organic piezoelectric materials.

(2) Semiconductor devices

At present, the mainstream of semiconductor devices comprise those made of silicon. However, where higher performance than available from silicon devices is required, compound semiconductors are used. Particularly, in the fields of optoelectronic devices or ultrahigh-frequency devices, silicon devices are not useful. If it is made possible to integrate compound semiconductor elements on silicon

substrates along with other elements made of silicon, devices with higher performance will be made available. However, since silicon and compound semiconductors differ in crystal lattice constant, compound semiconductors cannot be grown directly on silicon substrates. If it is made possible to form compound semiconductors in silicon substrates by using the MOCVD or MBE technique to make the substrate composition locally gradient, it will become possible to fabricate low-priced high-performance devices.

(3) Magnetic applications

In the field of magnetic disk memories, vertical recording has started to be made. The magnetic films used as recording media have a dual structure consisting of a soft base portion and a hard upper portion. When a magnetic material is subjected to stress, its characteristics deteriorate. Making the film composition gradient will enable the stress-susceptibility of the film to be reduced.

The permanent magnets or the cores of electromagnets used in motors, NMR's, etc. are required to have high saturation magnetic flux density. The parts to be made of a precious alloy of such magnets can be made smaller by improving their shapes. Their parts where magnetic flux density need not be high may be made of an inexpensive alloy. Thus, making the composition of magnetic material gradient according to the magnetic density flux requirement will make it possible to produce low-priced high-performance magnets.

(4) Application to sensors

Keeping pace with the progress of mechatronics and factory automation, a large variety of sensors has been developed and such sensors are required to meet increasingly severe requirements as to operating range and accuracy. Under such circumstances, semiconductor sensors and fine-ceramic sensors incorporating advanced technology are nearing the stage of practical use. There are however cases where sensors which meet specifications do not function according to specifications when actually attached to the objects of measurement. Such cases include those in which sensors are subjected to stress or temperature change when they are encased or are attached to the objects of measurement and result in suffering from drifting or noise. This type of case can be prevented from occurring by inserting a gradient-composition layer between sensor and mount.

Precision electric measurements to be made require the measuring terminals to be afloat. When measurements are to be made in a severe environment (where, for example, high temperature, high pressure, or corrosive gas is present), plastic parts or adhesives cannot be used. It is ideal that sensors to be used in such an environment consist of metallic and ceramic parts. However, metallic and ceramic parts cannot be joined by the conventional techniques. Sensors, like the one shown

in Figure 12, which can be used to measure the conductivities of high-temperature, high-pressure liquids can be produced using the gradient composition control technique.

It may be possible that a gradient composition functions as a sensor. If the composition of a sensor material can be controlled such that the sensor has spatially gradient sensitivity, it will be possible to let the sensor itself perform a function of information processing or to make the sensor capable of detecting more than one signal.

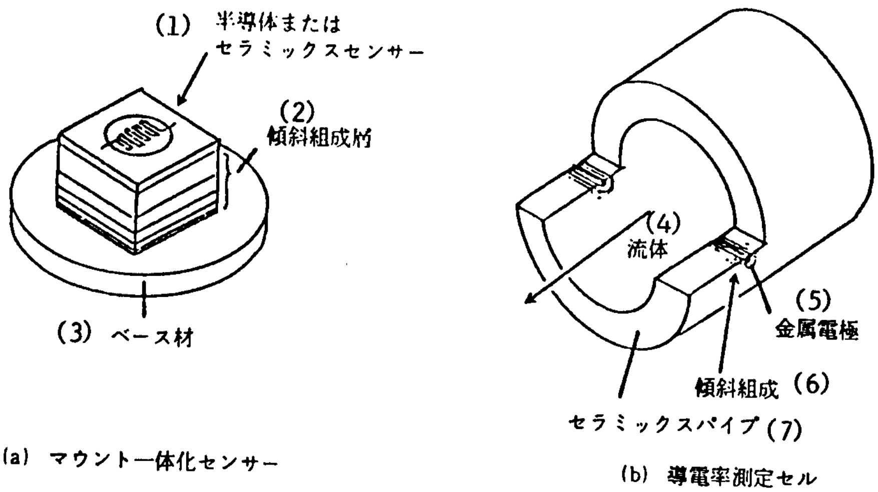

Figure 12. Sensors With Gradient Composition

Key:

(a) Sensor unified with mount
1. Semiconductor or ceramic sensor
2. Gradient-composition layer
3. Base material

(b) Conductivity measuring cell
4. Fluid
5. Metallic electrode
6. Gradient composition
7. Ceramic pipe

2.2.4 Functions for Optical Applications

The gradient composition control technique has been in use from before in the optical fields.

Multimode fibers used as transmission lines for optical fiber communications has a gradient composition so that their refractive index is the highest in their core and lower in their parts more away from the core. GRIN lenses [gradient index lenses] which are a kind of rod lens also have a distributed index, like multimode fibers, attributable to a gradient composition. Research work on optical waveguides and

microlenses to be manufactured by the ion exchange method is also being actively promoted.

In glass lasers produced by doping glass with Nd and used for laser-machining or laser fusion, the Nd concentration is distributed such that their luminous efficiency as well as cooling efficiency is optimized.

The composition gradients in the foregoing optical products are very small however.

It will be possible to develop new optical parts or optical memory devices using the gradient composition control technique to distribute the refractive indices of optical materials in larger gradients or to form electrooptic or magnetooptic materials inside optical materials.

2.2.5 Other Functions

(1) Functions for chemical applications

Research work on C_1 chemistry for synthesizing raw materials for use in the petrochemical industry from relatively simple-structured compounds using high-performance separation membranes and catalysts as well as that on chemical synthesis techniques for making selective reactions using laser is under way. Research for the development of bio-reactors which make use of fermentation or gene recombination techniques is also being made. The gradient composition control technique will be applicable to the development of membranes, catalysts, or reactor vessels mentioned above. Chemical plants to be built using such technique will be required to incorporate reactor systems different from the conventional ones. Reactor vessels and tubes made of complex materials discussed in the foregoing in connection with the material joining function may be used in such plants.

(2) Other application fields

Functionally gradient materials have a limitless potential as a means of solving problems attributable to interfaces between joined materials and also as a new type of materials whose gradient compositions themselves can perform a new function. They are expected to contribute to the development of higher-performance industrial apparatuses operable with less energy.

The objects of utilization of the gradient composition technique are not limited to such highly technical items as aeronautical and space equipment. It can also be applied to the production of common materials such as paper, fiber, clothing, food, and construction materials. Functionally gradient materials will also find applications in durable consumer goods and other articles for use in civilian life.

Utilization of functionally gradient materials will serve to quicken the development of new material production processes as well as new measurement control techniques. Thus, the introduction of functionally gradient materials is considered to be able to produce almost limitless effects. (See Table 2.)

3. Development of Functionally Gradient Materials for Thermal Stress Reduction

3.1 Aims of R&D

When conducting research for the development of a functionally gradient material for thermal stress reduction, it is essential to set concrete targets to be accomplished. Doing so will be instrumental in producing a greater result in a shorter period of time and enabling the developed technique to be quickly disseminated to associated fields.

Among the typical applications of functionally gradient materials to be developed for use in a severe thermal environment are space shuttles and fusion reactors. When attention is given to the process of material development, it is expected that assessing materials under development as to thermal stress generated in them and their heat blocking function will involve many difficulties.

Taking into account the above points and considering that verification of the functions of space shuttle materials is practicable in a simulated thermal environment, the author will discuss the targets to be set for material development on the assumption that the material to be developed is for use in a space shuttle. The maximum performance values achieved by presently available ultraheat-resistant materials for aeronautical and space applications are listed in Table 3. In Figure 13, the temperatures estimated to be reached on various parts of the surface of a space shuttle as well as in its propulsion system are indicated. For the present study, the final goal has been set as developing 1-10 mm thick material capable of withstanding a surface temperature of 2000 K and a temperature head of 1000 K.

Table 2 Expected uses, other than for thermal stress reduction, of functionally gradient materials

Expected function	Applications	Composition and expected effects
- Nuclear function	First wall and peripheral devices (limiters, divertors)	Radiation resistance, thermal stress resistance, low Z
	Electric insulators (for torus structures, superconductors)	Electric insulation
	Plasma measurement and control window materials	Light transmissibility, radiation resistance
- Joining function	Ceramic engines, abrasion-resistant, heat-resistant, or corrosion-resistant mechanical pars, other mechanical parts	Ceramic and metal Glass and metal Plastic and metal Different metals Different ceramics Different plastics
		Materials which were not formerly joinable can be tightly joined
- Medical or organismic function	Artificial teeth Artificial bones Artificial joints	Pore distribution control for ceramics Ceramic and plastic Ceramic and metal
	Artificial organs	Gradient-composition control for organic materials for living bodies
		Greater adaptability to living bodies and higher functional reliability
- Electric or magnetic function	Ceramic filters Ceramic oscillators Ultrasonic vibrators Magnetic disks Permanent magnets, electromagnets 3-dimensional composite electronic parts Silicon and compound semiconductor hybrid IC's Long-life heaters	Gradient composition for piezoelectric materials Gradient composition for magnetic materials Gradient composition for metals Silicon and compound semiconductor
		Characteristic improvement and weight and size reductions

- Sensor function	Sensors unified with mount Acoustic sensors matching with media Sonars, ultrasonic diagnostic systems Sensors with spatially distributed sensitivity	Gradient composition between sensor and mount materials Gradient composition for piezoelectric materials
		Measurement accuracy enhancement, measurement in severe environment
- Optical function	High-performance laser rods Large GRIN lenses	Gradient composition for optical materials
	Optical disks	
		High-performance optical parts
- Chemical function	Functional macromolecule film catalysts	Metals, ceramics, plastics, glass, proteins, cement
- (Civilian fields)	Paper, fiber, clothing, food, construction materials	

Table 3. Present Level of Ultraheat-Resistant Materials and Development Target Set for Present Study

Level	Ultraheat-Resistant Heat-Blocking Material	Ultra-Resistant Heat-Shielding Structural Material
Target	Thickness: 1 to 10 mm Surface temperature: 2000 K Temperature head: 1000 K	
Present	(Main engine for space shuttle) Thickness: 1 mm Surface temperature: 800 K Temperature head: 300 K (Gas turbine engine) Thickness: 1 mm Surface temperature: 1400 K Temperature head: 500 K	(Heat insulating tiles for space shuttle) Thickness: 100 mm Surface temperature: 1600 K Temperature head: 1600 K

In the United States, the Office of Science and Technology policy (OST) came out, early in 1986, with a long-range plan for aeronautical and space development with an eye set on the 21st century. In the plan, ultraheat-resistant material techniques are defined as extremely important fundamental techniques for the development of space shuttles. Basic research work for the development of ultraheat-resistant materials based on the plan is already in progress. In the light of such a situation, now will be the appropriate time for Japan, from an international point of view, too, to start R&D on fundamental techniques for the development of materials usable in aeronautical and space applications based on a long-range standpoint.

3.2 R&D System

In proceeding with R&D on materials, it is necessary to maintain a system in which three departments, that is, for material design, structure control, and characterization, respectively, are organically interrelated to enable relevant information to be fed back and forth between them. In such a system, when a material to be developed is determined, the design department is to start 0th design.[6)] The term 0th design is used because, without any functionally gradient material synthesized of specific raw materials being available at present, initial design cannot but be dependent on estimates to be made based on

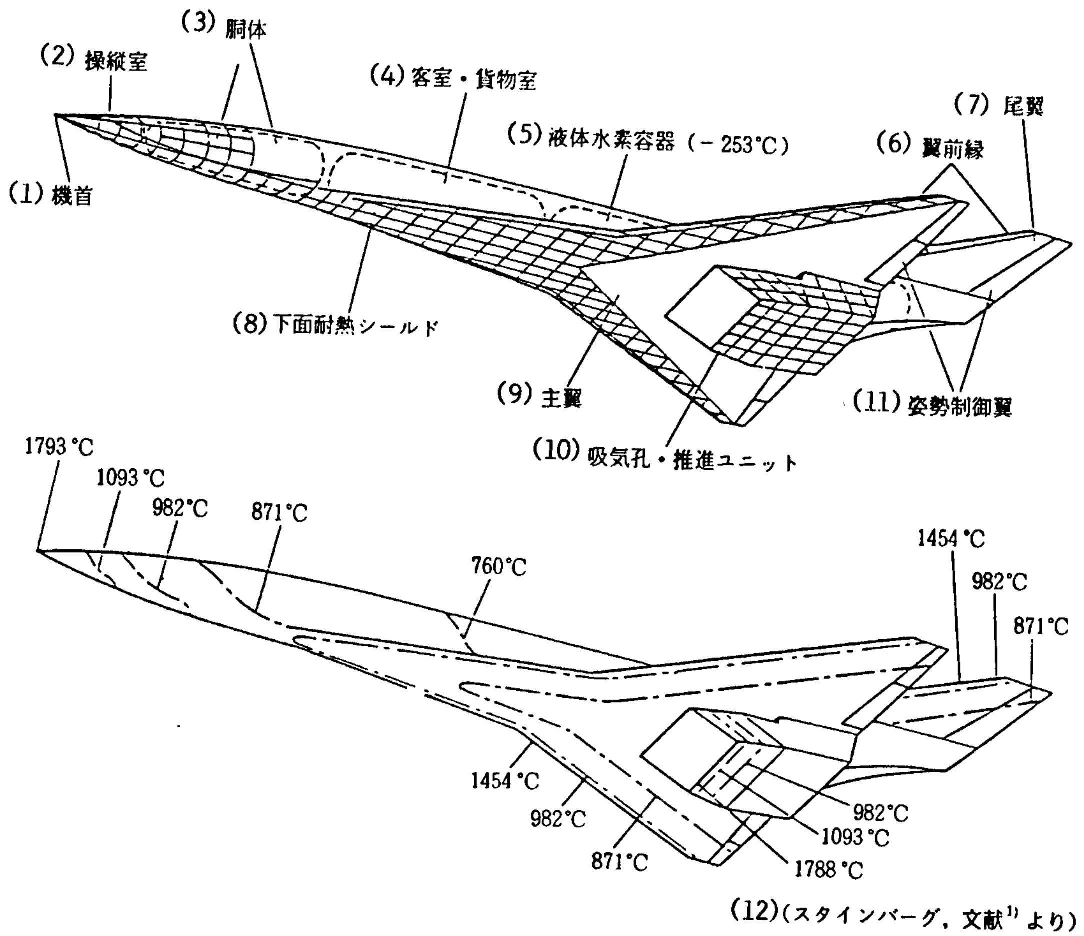

Figure 13. Temperatures at Different Parts of Space Shuttle

Key:

1. Nose
2. Cockpit
3. Fuselage
4. Passenger cabin and cargo compartment
5. Liquid hydrogen container
6. Wing front-edge
7. Tail
8. Bottom heat-resistant shield
9. Main wing
10. Air suction port and propulsion unit
11. Attitude control fin
12. (Steinberg)

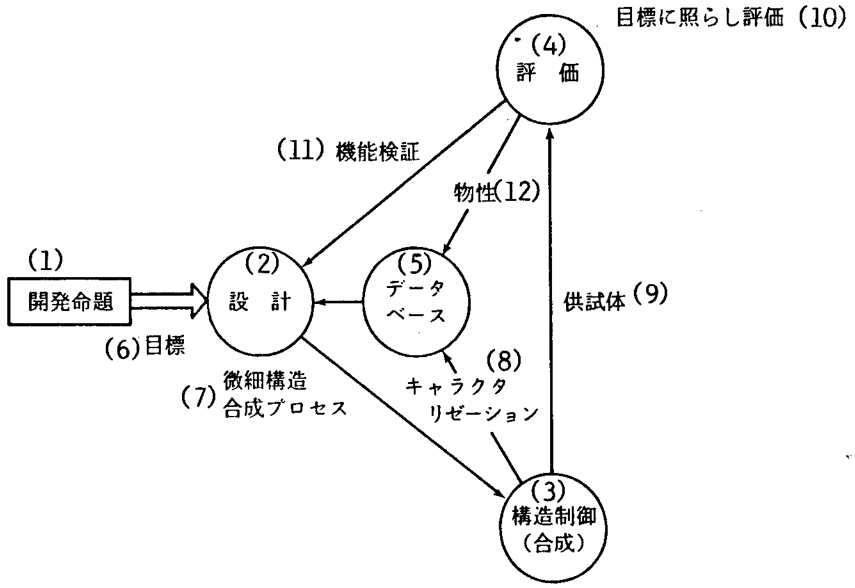

Figure 14. R&D System

Key:

1. Development plan
2. Design
3. Structure control (synthesis)
4. Assessment
5. Data base
6. Target
7. Microstructure synthesis process
8. Characterization
9. Samples
10. Assessment made with targets taken into account
11. Function verification
12. Physical properties

existing data and empirical laws which appear most suitable for adoption. When information on the microstructure of the material to be developed and the synthesis process to be used is received from the design department, the structure control department is to proceed with the manufacture of small samples of nongradient (homogeneous) material in widely varying compositions. Subsequently, the assessment department is to assess various characteristics of the samples prepared by the structure control department and thereby build up a special data base which can be used in designing structurally gradient materials. Only after the data base is prepared, it becomes possible to make the 1st design for developing a functionally gradient material.

At the same time as giving the microstructure and synthesis process information to the synthesis department, the design department is to also forward information on the assessment methods and criteria used in the design stage to the assessment department. The assessment methods and criteria are to be used to assess the samples as to, for example, thermal stress, heat blocking performance, thermal gradient properties, thermal fatigue life, and thermal shock characteristic.

Thus, until the targeted functionally gradient material is developed, materials and information are exchanged among the three departments in charge of design, synthesis, and assessment, respectively, forming a closed loop centered around a data base.

3.3 Objectives of R&D and Course of Development

The objectives of material research to be given priority in this country and the expected course of development of such research work are listed in Table 4. The contents of the table reflect the results of a survey made to assess the present status of techniques for material design, structure control, and characterization and to consider what objectives are to be set in this country in proceeding with the development of functionally gradient materials.

(1) Material design

-1 Development of intelligent retrieval system for functionally-gradient material property data;

-2 Development of techniques for analyzing multidimensional thermal stress and macroscopic deformation;

-3 Development of design system in which data and theories on functionally gradient materials are integrated.

With regard to material design, the above three priority objectives have been set. At first, 0th design is to be made based on a data base containing data on existing homogeneous materials. Gradient-property data are to be collected through the subsequent research work made based

Table 4. Objectives of R&D and Course of Development

Material Design

-- Development of intelligent retrieval system for functionally-gradient material property data
-- Development of techniques for analyzing internal thermal stress and macroscopic deformation
-- Development of multidimensional thermal stress analysis method
-- Development of design system in which data and theories on functionally gradient materials are integrated

Microstructure synthesis process

Characterization

Structure Control

-- Techniques for controlling composition, precipitation phase and pore distributions by physical or chemical vapor deposition method
-- Techniques for packing and arranging different types of multifunction powders with gradient compositions and sintering them
-- Techniques for lamination forming by plasma-spraying and precision enhancement
-- Technique for composition control by self-exothermic reaction method

Establishment of combination techniques

Preparation to meet needs for larger materials

Samples

Characterization

-- Technique for quantitative assessment of local thermal stress
-- Technique for overall assessment of thermal and mechanical strength of functionally gradient materials
-- Technique for overall assessment of heat blocking performance of functionally gradient materials

Property and function verification

Assessment method and criteria

To material design

From material design

on the results of the 0th design. The collected data are to be accumulated and used to improve the material design accuracy in stages until a system for designing one-dimensional gradient compositions based on steady-state heat conduction is created. In the next step, unsteady-state models are to be incorporated in the design system. They are to be eventually expanded into three-dimensional gradient models for large-scale structural materials. It is also necessary to introduce the concept of pre-strain as a means of effectively reducing thermal stress. For gradient-model verification, it is necessary to make positive use of the fruits of research work on thermal stress quantification made using functionally gradient plastics. Such an approach will be instrumental in establishing the design concept for functionally gradient materials totally different from the conventional material design concept used to pursue material homogeneity.

(2) Structure control

-1 Techniques for controlling composition, precipitation phase and pore distributions by physical or chemical vapor deposition method;

-2 Techniques for packing and arranging different types of multifunction powders in gradient compositions and sintering them;

-3 Techniques for lamination forming by plasma-spraying and density enhancement;

-4 Technique for composition control by self-exothermic reaction method.

With regard to structure control, the above four priority objectives have been set. At first, it will be necessary to test-manufacture nongradient (homogeneous) materials with widely varying compositions in order to enhance the data base. In the next step, small-scale experiments should be made on each elementary technique so that various fundamental problems with regard to gradient composition control may be revealed. The pore distribution control technique and temperature-difference forming technique also make up important objectives to be achieved. The synthesis method considered comprises, in a broad sense, two techniques, one for phase distribution control as mentioned in -1 and the other for controlling particle arrangement. With regard to the phase distribution control technique, precipitation speed enhancement should be a target to be achieved. The particle arrangement control technique should be aimed at making thinner materials producible. More concretely, realization of material thicknesses of 1 to 10 mm should be aimed at; this thickness range is not covered by the present technique but it is the most required range of thickness for practical purposes. Larger-scale experiments should subsequently be carried out by taking into account the results of small-scale experiments. The major objectives for which large-scale experiments are to be made should include techniques for obtaining three-dimensional gradient

compositions, for enlarging gradient-composition parts, and for real-time structure control to be made with an aid of a computer linked with a design system. It is inevitable that, in the process of upgrading material synthesis techniques, various elementary techniques are fused or combined as required. Samples measuring as large as 300 by 300 mm or having complicated shapes can be produced only after the foregoing techniques are established.

(3) Characterization

-1 Technique for quantitative assessment of local thermal stress;

-2 Technique for overall assessment of the thermal and mechanical strength of functionally gradient materials;

-3 Technique for overall assessment of heat blocking performance.

With regard to characterization, the above three techniques have been selected as the priority objectives.

The technique mentioned as -1 constitutes the only means of directly verifying gradient material design models. This technique should be established in an early stage in order to enable the material development being discussed to be expedited.

As for the techniques mentioned as -2 and -3 above, local distributions of various thermal and mechanical properties of the small testpieces to be received from the synthesis department are to be measured and assessed in the light of development targets. Subsequently, various tests including basic tests with high temperature heads and simulated environmental tests are to be made based on the results of the above measurements. The assessment department is also to screen various materials according to the assessment criteria prepared by the design department and thereby to contribute toward gradually improving the techniques for material design and structure control and facilitating the efficient promotion of material development.

The assessment department is, furthermore, to carry out assessment tests in simulated environments such as hot-gas flowing fields, aerodynamic-heating fields and fast rotation fields. The results of such tests are to be used as the basis for ascertaining the overall functions of the materials developed as structural elements. Furthermore, it should also be aimed to establish, based on the test results, the basic guidelines for creation of the material selection, safety examination, and design criteria to be referred to when planning practical applications of functionally gradient materials.

BIBLIOGRAPHY

1. Steinberg, M.A., (translation by Nakagawa, Y.) "SAIENSU," Nikkei Science Inc., p 29, Dec 1986.

2. Niino, M., et al., "Functionally Gradient Material Production Method," Japanese patent application No. 60-297042, 1985.

3. Kawasaki, A., et al., Proceedings of autumnal meeting of powder metallurgy association of Japan [Funtai Funmatsu Yakin Kyokai], Nov 1986.

4. Sada, N., et al., Texts for 25th discussion of fundamental ceramics, Jan 1987.

5. Niino, M., et al., "Functionally Gradient Material Production Method," Japanese patent application No 61-187370/1986.

6. Hirano, T., et al., Texts for material mechanics association lecture meeting, Nov 1986.

20109/09599

Defense Agency Reports on Materials, Systems Summarized

Gunpowder and Intragun Trajectory

43062532a Tokyo BOEI GIJUTSU in Japanese Sep 87 pp 51-53

[Report by Yoshitaka Hara, student, Material Engineering Faculty, Defense Academy: "Study of High-Pressure-Index Gunpowder and Intragun Trajectory Curve"]

[Text] 1. Preface

The nitramine-based propellant offers advantages, such as low average molecular weigh of combustion gas and large gunpowder power. However, due to its disadvantage of a high pressure index, its practical use has been limited. For this reason, this laboratory tried several methods to lower the pressure index of the propellant, but has not yet obtained satisfactory results.

This study is not a challenge to lower the pressure index but, instead, a trial to derive an effective pressure-generating process by making use of the high pressure index and manipulating gunpowder shapes. Further extension of this way of thinking suggests possible application to the movable loading gun system which is now attracting attention.

2. Study

(1) Pressure indexes of propellants

Figure 1 shows actually measured values of relationships between the pressure and combustion speed of the propellants currently being used, M1 and M30, and nitramine-based propellants, F1 and F2. Nitramine-based propellants have lower combustion speeds below a certain pressure when compared with the propellants currently being used. Above this pressure, however, the former propellants show very high combustion speed as the pressure increases. This causes abnormally high pressure when they are used in the powder chamber of a gun in a half-sealed state.

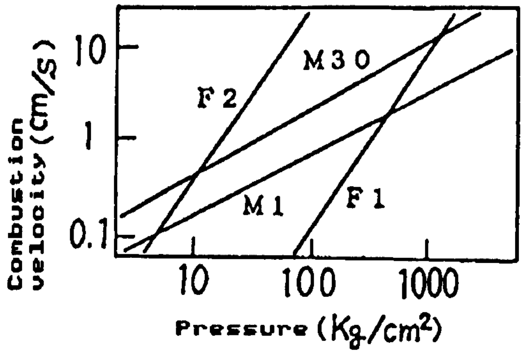

Figure 1.

(2) Shape of intragun pressure-shell travel curve

Figure 2 shows the shape of the intragun pressure-shell travel curve when a wing-stabilized shield-penetrating shell with a loading tube (APDS-FS) is discharged by the main gun of a 74-type tank. The area enclosed by this pressure curve is the work quantity which acts on the shell and is converted to the shell's kinetic energy. For increasing the muzzle velocity, therefore, the area enclosed by the pressure curve needs to be made still larger.

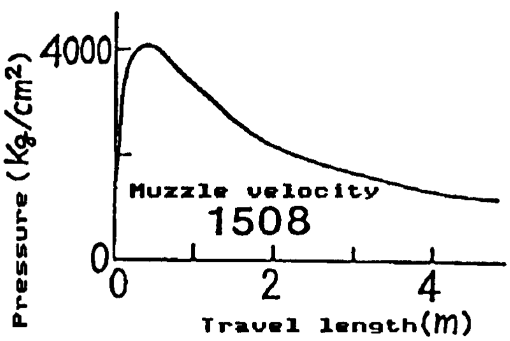

Figure 2.

Ideally speaking, the maximum pressure should be maintained after it has been reached. At the time a shell has been accelerated and is traveling, the pressure generation compensating for the volume expansion due to the shell speed is thought to be necessary. In such a case, the high pressure index of the nitramine propellant may be utilized

(3) Application of two-layer gunpowder grains of different combustion speeds

Figure 3 shows a model explaining the idea mentioned above.

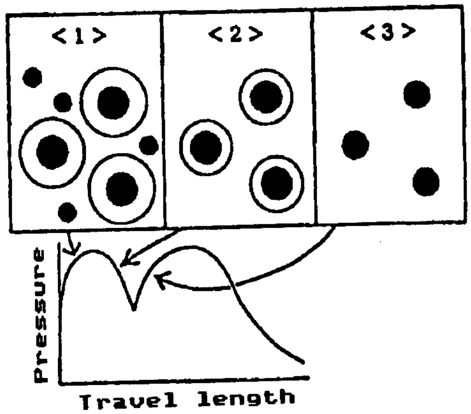

Figure 3.

In the above figure, black-circle parts show nitramine-based propellant and white-circle parts show the current propellant. In addition, smaller black circles show fine grain of nitramine-based propellant.

a. Combustion of fine grains causes the first-step pressure rise and the maximum pressure to be reached.

b. Although white external-layer gunpowder is still burning, even after combustion completion of fine grains, this burning is not fast enough to maintain the maximum pressure. Therefore, the pressure of the powder chamber drops temporarily.

c. When the nitramine-based propellant in inside layers starts combustion, another pressure rise occurs at a speed that exceeds the acceleration of the shell, causing the second-step maximum pressure.

Since the above-mentioned two-hill pressure curve should enclose a larger area than the conventional one-hill pressure curve does, an equivalent increase in the shell velocity is expected.

3. Intragun trajectory computation

(1) Loading two kinds of grains--two layer and fine grains

A trajectory-computing program, which follows the above-mentioned model, was coded, and intragun trajectories were computed (nitramine-based propellant: F1, current propellant: M1). At this time, kinds of two-layer gunpowder were increased from one (Figure 4) to three (Figure 6). Therefore, pressure curves, which maintain maximum pressure horizontally, could be selected. as a result, a muzzle velocity, which was higher by 7 to 9 percent than that of he conventional 74-type APDS-FS, was obtained.

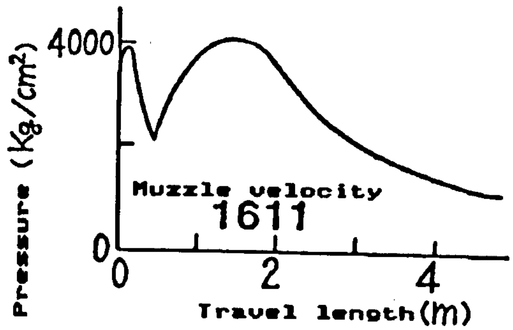

Figure 4.

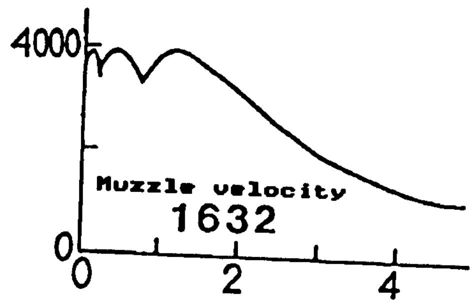

Figure 5.

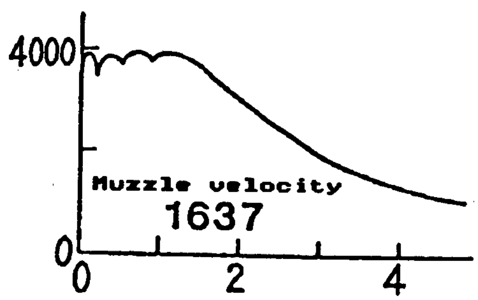

Figure 6.

(2) Two-layered movable gunpowder

Since the nitramine-based propellant F2 exhibits fast combustibility at high pressure, it will be usable for movable loading if two-layer processing is used.

Trial combustion was made by replacing half the quantity of the current propellant of the 74-type tank with two-layered movable gunpowder (internal-layer gunpowder: F2) (Figure 7). This manipulation increased the muzzle velocity by 20 percent, compared with the conventional one.

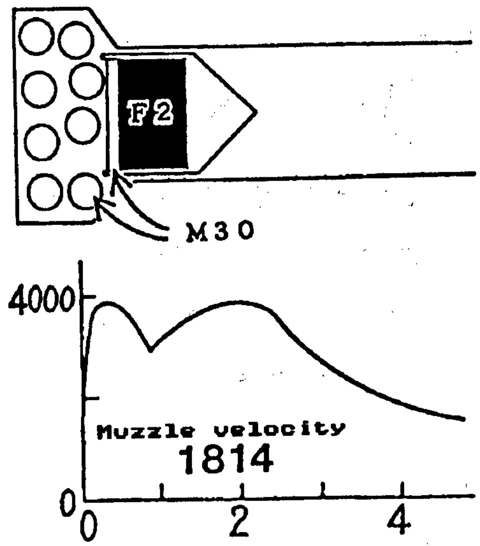

Figure 7.

Advisors: Professor Takeshi Ito
Assistant Professor Yutaka Hagiwara

BIBLIOGRPAHY

1. Hironori Ono, Graduation Thesis, Science and Technology Research Course, Defense Academy 1985.

2. Yasushi Tashiro, Sukeyasu Katagai, and Nobuyoshi Tan, "Technical Report," Technical Research Headquarters, Defense Agency, Tech-376, 1969.

3. Yasushi Tashiro, Sokumichi Arizono, and Nobuyoshi Tan, "Technical Report," Technical Research Headquarters, Defense Agency, Tech-504, 1972.

Reinforced Concrete Beam's Tolerability

43062532a Tokyo BOEI GIJUTSU in Japanese Sep 87 pp 53-54

[Report by Ichiro Yamada, student, Structural Dynamics Faculty, Defense Academy]

[Text] 1. Preface

(1) General properties of members subject to dynamic loads

Properties of concrete members subject to impact loads differ from those of concrete members subject to static loads. This is due to the influence called velocity effects, which include increases in strength and changes in strain and modulus of elasticity. These changes in properties cause changes in the strength of structures and the quantity of deformation.

(2) Purpose of this study

The blastproof design of a structure subject to blast pressure has been calculated in sections by making the blast pressure equal to the absorption energy, which is the product of the critical deformation quantity of the structure and the maximum proof stress. However, determination of the design deformation quantity when a safety factor is taken into consideration is not clear. Therefore, this study explains the critical performance items, such as critical deformation quantity and maximum proof stress, of the beams which are subject to dynamic loads and examines the safety margin of the blastproof design.

2. Experiments

(1) Experiment device and loading velocity

A high-speed loading device was used. Loading was accomplished by rapidly displacing an actuator from the state in which a bar-like loading body was contacting a sample. The sample was simply supported. The sampling time of the experiment data was set to 0.5 s for static loading and 0.2 ms for dynamic loading. The loading velocity in the static experiment was about 0.024 cm/s, and that in the dynamic experiment was about 60 cm/s, about 2,500 times that in static experiment.

(2) Sample

Twenty samples were made. These included single iron-rod reinforced concrete beams with two iron rods (D10 [0.53 percent], D13 [0.94 percent], D16 [1.47 percent]) on tension sides (static: 3; dynamic: 5) and double iron-rod reinforced concrete beams with equal quantities of iron rods (D10, D13, D16) on both the tension and compression sides (static: 5; dynamic: 7). The shear reinforcement iron rod is of 6 ϕ at 8 cm. The span length is 150 cm for the single iron-rod reinforcement and 130 cm for the double iron-rod reinforcement. The average compressive strength of the concrete was 304 kg/cm^2, and the average tensile strength of the iron rod was 3,658 kg/cm^2. [Brackets within paragraph as published]

(3) Results

a. Single iron-rod concrete beam

The final deformation quantity was assumed to be the deformation quantity at the middle point, which corresponds to the point at which the load rapidly decreased. The final deformation quantity decreases as the reinforcement ratio increases for both the static and dynamic tests. The final dynamic deformation quantity increases by about 20 percent against the final static deformation quantity. The maximum proof stress rises with an increase of the reinforcement ratio. The maximum dynamic proof stress resulted in an increase of about 25 percent, compared with the maximum static proof stress. The absorption energy is defined as the product of Pu (maximum proof stress) and Xm (final deformation quantity). The static absorption energy becomes maximum when the reinforcement ratio is about

1 percent. The dynamic absorption energy showed an increase of about 45 percent against the static absorption energy.

b. Double iron-rod reinforced concrete beam

The final deformation quantity increases as the reinforcement ratio increases both for static and dynamic tests. The final dynamic deformation quantity increases by an average of 20 percent against the final static deformation quantity. When the reinforcement ratio is 0.53 percent, reinforcement ruptured in both static and dynamic tests, with the final dynamic deformation quantity being about the same as the final static deformation quantity. The maximum proof stress increases as the reinforcement ratio increases in both static and dynamic tests. The maximum dynamic proof stress is larger by an average of 10 percent than the maximum static proof stress. The absorption energy increases as the reinforcement ratio increases. The dynamic absorption energy is larger than the static absorption energy, except for the reinforced concrete beam of reinforcement ratio of 0.53 percent.

3. Analysis and minimum reinforcement ratio

(1) Absorption energy by calculation (Table 1)

The final deformation quantity was calculated on the assumption that the bending moment increases at a fixed rate from the crack moment to the final moment, and the angle of rotation is the integral from the curvature by the crack moment to the final moment. Also, yield proof stress was used in place of the maximum proof stress for safety. The yield proof stress and final proof stress are defined as shown above, and the absorption energy is defined as the product of Py and δu. When calculated values are compared with the experimental values, all the calculated values are on the safe side.

Table 1. Absorption Energy

Reinforcement ratio		0.53	0.94	1.47
Single reinforce-	Experiment result	51.2	59.2	57.3
	Absorption energy by this method	17.2	31.8	39.4
	Real value/value by this method	2.90	1.86	1.45
Double reinforcement beam	Experiment result	29.2	72.6	113.5
	Absorption energy by this method	13.8	37.0	79.3
	Real value/value by this method	2.11	1.96	1.43

(2) Minimum reinforcement ratio free of brittle fracture (Table 2)

The standard concrete specifications show the minimum reinforcement ratio. In this experiment, however, the minimum reinforcement shown in the specifications is sometimes inconvenient. When the tensile reinforcement ratio is small and double reinforcement ratio is large, ductility becomes small and absorption energy becomes smaller than that of the single reinforcement. Therefore, the minimum reinforcement ratio has been determined so that the tensile reinforcement does not rupture, on the assumption that the final strain of the tensile reinforcement will be 10 percent.

Table 2. Sample Minimum Reinforcement Ratio Calculation

Reinforcement ratio		Minimum reinforcement ratio	$\frac{\text{Double absorption energy}}{\text{Single absorption energy}}$
0.53	$r = 1$	0.70	On the average of 0.73
0.94	$r = 1$	0.85	On the average of 1.30
1.47	$r = 1$	1.06	On the average of 2.10

4. Conclusion

(1) The single-rod reinforced concrete beam shows a small rise in blastproof performance when the tensile reinforcement ratio is 1 percent or more.

(2) The absorption energy of a reinforced concrete beam, that does not cause local fracture when subjected to dynamic load, has come to be estimated fairly safely.

(3) When the tensile iron rod quantity is the same as the compressive iron rod quantity, the absorption energy is larger for a double iron-rod reinforced concrete beam than for a single iron-rod reinforced concrete beam if the tensile reinforcement ratio is larger than the minimum reinforcement ratio and smaller than the balanced reinforcement ratio.

Advisor: Professor Takashi Uchida

BIBLIOGRAPHY

1. Yoshio Kosaka and Shiro Morita, "Reinforced Concrete Structure," Maruzen, 1978.

2. Hiroshi Yamaguchi, Kazuo Fujimoto, and Setsuro Nomura, "Dynamic Response Analysis of Reinforced Concrete Beams Subject to High Loads," STRUCTURE ENGINEERING PAPERS, Vol 328, March 1986.

Supersonic Image Pickup System

43062532a Tokyo BOEI GIJUTSU in Japanese Sep 87 pp 54-57

[Report by Hironobu Ikemoto, student, School of Electronics Engineering, Defense Academy: "Study of Supersonic-Wave Image Pickup System Using Leaking Lamb Wave Device"]

[Text] 1. Preface

Recently, a technique which nondestructively investigates the internal state of an optically opaque substance has been attracting attention. The technique, using supersonic waves, is particularly thought of as a powerful observation method.

The setup of bamboo-blind-like electrodes in a piezoelectric substance sheet composes a transducer capable of transmitting and receiving Lamb waves. If this Lamb wave device is made to contact a liquid, supersonic waves can be excited in the liquid. In this study, a supersonic image pickup system has been constructed with a device which has four bamboo-blind-like transducers (IDTs) on one surface of a piezoelectric sheet, and image pickup is attempted by devising image processing. This article reports on the principle of operation, the experiment system, and the results obtained.

2. Principle

If RF pulses are introduced into the wave-transmitting IDT of the Lamb wave device as shown in Figure 1, underwater supersonic waves are radiated in the direction of angle θw. The supersonic waves propagate under water, reach the test piece, and are reflected on the surface. The remaining supersonic waves enter the inside of the test piece in accordance with Snell's Law, but are reflected at acoustically discontinuous places. These reflected waves propagate water layers again and are converted to electric signals by the receiving IDT. The signals obtained via such a process are those which have been modulated by the elastic characteristics of the surface and inside of the test piece. Therefore, if these signals are appropriately processed, nondestructive acoustic images are obtainable. In this study, four arc-shaped IDTs are grouped into two facing pairs and these pairs are positioned perpendicularly to each other to improve resolution.

3. Experiment method

Figure 3 shows the configuration of the experiment system. Delay signals at the receiving IDT contain multiple reflected waves and unnecessary signals, depending on the paths of the sound waves. To take out only the desired signal components, a synchronized analog switch is used. Figure 3 shows a sample observation of input and output wave forms to and from the Lamb wave device and the gate signal to drive the analog switch. In this case, the gate position has been selected so that signals of maximum amplitudes can be taken out.

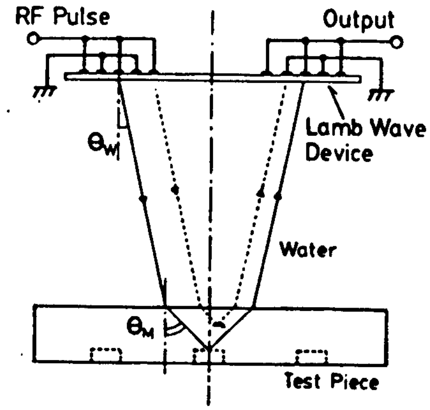

Figure 1. Propagation Paths of Lamb Wave Device and Sound Waves

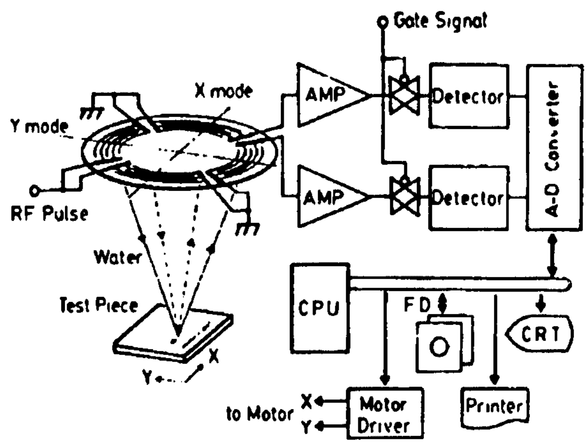

Figure 2. Image Pickup System Concept

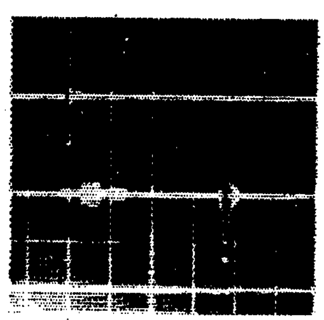

Figure 3. Waveforms of Input-Output Signal and Gate Signal

For the device substrate, the piezoelectric ceramic NEPEC-6 (manufactured by Tohoku Metal Industries, Ltd.) is used, and IDTs have been designed so that superior operating characteristics are obtained together with superior conversion efficiency. To be more concrete, an arc-shaped bamboo-blind-like electrode, with a period length of 430 μm and consisting of 35 pairs

is set up on the dry surface of the substrate with diameter and thickness of 14 mm and 220 μm, respectively.

The test piece for the experiment is a copper plate, 40 mm x 30 mm x 1 mm, and its back surface has etched grid-like grooves of pitch 1 mm, as shown in Figure 4, to the depth of about 100 μm.

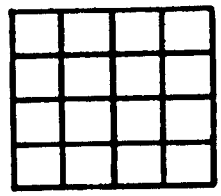

Figure 4. Grid

4. Results of experiment

Figure 5 shows a concrete example of the acoustic image obtained by using the above-mentioned experiment system. In this figure, (a) corresponds to the reflected waves in the surface area and (b) corresponds to those reflected inside, in the area including the grid.

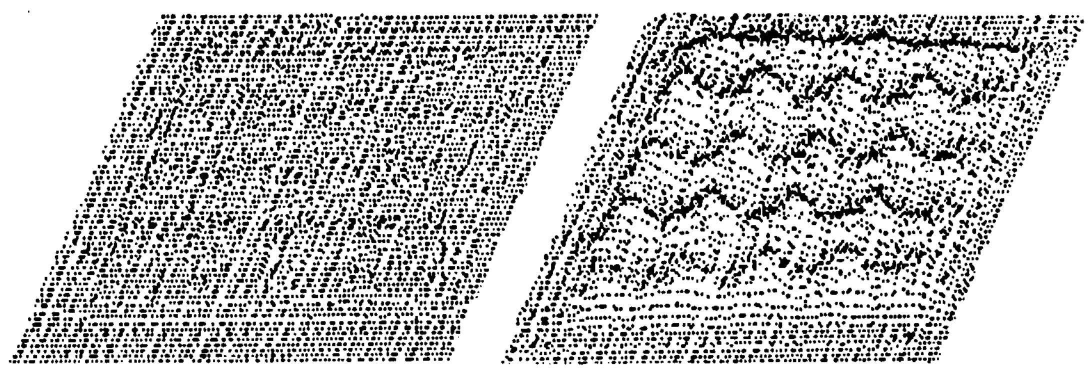

(a) Surface area **(b) Inside**

Figure 5. Acoustic Image

In obtaining an acoustic image, the method of signal processing can be selected. That is, of four arc-like IDTs, two input IDTs can be used so that propagation directions of sound waves are perpendicular to each other. At this time, the sound wave direction is made to coincide with the X or Y direction, with the acoustic image obtained by the former called the X mode and that obtained by the latter the Y mode. (a) and (b) in Figure 6 show the X and Y modes corresponding to Figure 5. In this case, the images have been made two-dimensional by setting a threshold value. Figure (c) shows the result of superimposing the X- and Y-mode images. Figure (d) is the image obtained by multiplying the output values in the X and Y modes. When the X or Y mode exists alone, the compass-direction resolution can be improved in one direction, but two dimensionality poses a problem. This

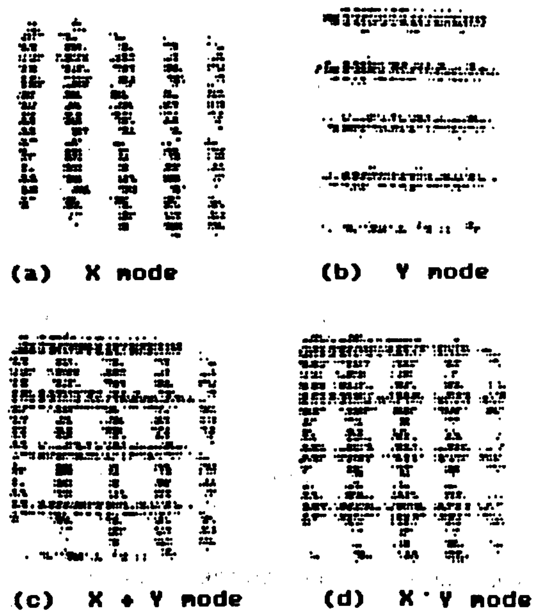

Figure 6. Correspondence Relationships of Acoustic Image

corresponds to (a) and (b). Obviously, such a problem has been improved by addition or multiplication processing.

5. Summary

An image pickup system has been constructed by using two pairs of perpendicularly placed arc-like IDTs and the addition or multiplication processing of two pairs of signals. As a result, the compass-direction resolution has been enhanced. This system shows that elastic discontinuity of the same degree as that of the wavelength can be detected, but experiments are being continued to further enhance image quality.

Advisor: Professor Koji Toda

BIBLIOGRAPHY

1. Ash, E.A. and Hill, C.R., Ed., "Acoustical Imaging," Plenum Publishing Corp., New York, 1982, Vol 12, p 125.

2. Hayama, M., and Toda, K., "An Acoustic Imaging System by Use of a Lamb Wave Device," JPN. J. APPL. PHYS., 22, Supp., 22-2, 1983, p 137.

Characteristics of Wind Tunnel

43062532a Tokyo BOEI GIJUTSU in Japanese Sep 87 pp 57-59

[Report by Hideki Kaba, student, Aeronautical Engineering, Defense Academy: "Study of Dynamic Characteristics of Low-Temperature Wind Tunnel"]

[Text] 1. Preface

The low-temperature wind tunnel, which has been attracting attention the past 10 years or so, has become required for us as a high-Reynold's wind tunnel, the method of confirming the dynamic similarity of which has become the base of the model test. The background includes the supply of required aerodynamically appropriate design data, as not only recent aircraft and space shuttles but also industrial products, such as high rises and large navigating machines, have become large and high-speed.

The main characteristics of such a wind tunnel are that the temperature of the gas inside the wind tunnel is as low as 100 K (-160°C to -170°C), that a high Reynold's number is obtained with the accompanying drop of dynamic viscosity of the air current, and that three independent control variables, including the internal pressure of the wind tunnel and the blower rotation speed, are obtained, and the Reynold's number, Mach number, and dynamic pressure can be changed by appropriately controlling these variables.

This article reports the results of the partial automation attempted by adding device revision to last year's manual operation method during the low-temperature wind tunnel operation method established at this academy, and compares the flow rate distribution on the measurement section and the static pressure on measured wall surfaces, obtained from many measurement points at normal temperature, with those in the previous report. This article also reports the new measurement related to the boundary layers on side walls.

2. Experiment device and method

This wind tunnel is a circulation-type low-temperature wind tunnel which takes in LN_2, corresponding to the heat occurring from the heat conduction and in blowers and wind paths, from the injection nozzle on the upper stream of the fan, and discharges the same quantity of gas to the outside from the exhaust port. The internal pressure of the wind tunnel is adjusted by opening and closing the valve at the exhaust port, but the previous manual valve has been replaced an automatic valve. As a result, the internal pressure has come to be controllable to the initially set pressure value.

Figure 1 shows the wind tunnel concept and Figure 2 shows the block diagram, indicating the correspondence between the feedback control system and the devices of this wind tunnel. Subject to external disturbance and load are changes in the LN_2 quantity and the number of fan rotations (air current velocity). Table 1 shows seven cases that occur when the PID values are changed properly.

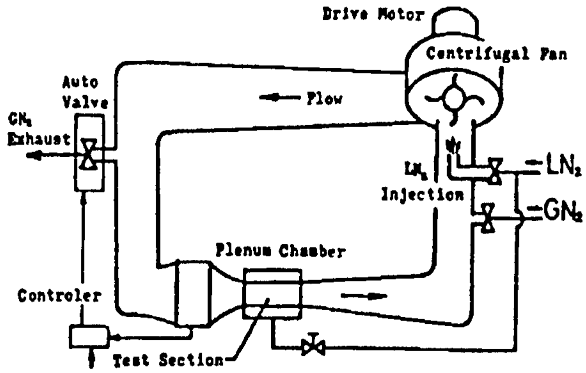

Figure 1. Low-Temperature Wind Tunnel Concept

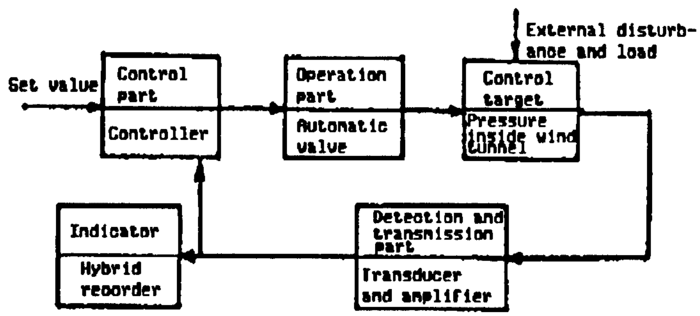

Figure 2. Feedback Control System

Table 1. PID Values and Stable Time

Case No.	①	②	③	④	⑤	⑥	⑦
P(%)	100	100	100	200	50	50	100
I (sec)	15	15	15	15	15	5	5
D(sec)	3	10	20	20	20	5	0
t_1(min)	3.0	3.0	3.0	—	2.5	2.5	3.1
t_2(min)	2.5	2.5	—	4.5	2.0	1.5	2.1

The upper and lower walls of the measurement part (300 x 720 x 60 mm) are slit walls with two grooves, and a diffuser flap is provided on the immediate lower stream. The relationship between the flap opening and the static pressure distribution on the side walls and the flow rate distribution on the measurement part section, where 217 measurement points have been set up, are measured with Pitot tubes and hot-wire current members.

3. Experiment results and ideas

Table 1 shows PID values and stable time t_1 and t_2. The set pressure was changed in the range from 1,100 kg/cm² to 1,250 kg/cm². Mutual comparison of individual cases yields the following results:

i) (2) and (4) show that the proportional band exerts great influence.

ii) (1) to (3) show that the derivative value (D value) seems to exert little influence on control in this case.

iii) Comparison of (5) and (6) and comparison of (2) and (7) in the same proportional band show that when the derivative time (I value) is set to from 15 s to 5 s, the time is shortened by about 30 s only when the pressure is set downward.

Figure 3 shows the changes of typical cases (2) and (6), as recorded by a hybrid recorder.

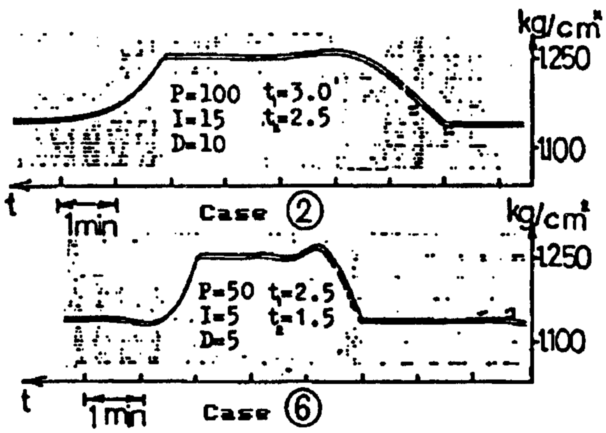

Figure 3. Changes of Pressure Inside Wind Tunnel With Time

Figure 4 shows the static pressure distribution on the wall surface of the measurement part during normal-temperature operation. This figure shows the influence by the flap opening on the pressure gradient on the lower stream. The pressure distribution should be as flat as possible from the upper stream of the measurement part to its lower stream, and the pressure gradient should be gradual on the lower stream. Therefore, the appropriate flap opening ranges from 25 to 30 mm.

Figure 5 shows the wall-surface Mach number distribution calculated from the wall-surface static pressure of the measurement part of this wind tunnel, and that of the Aeronautical Technology Research Institute's wind tunnel.

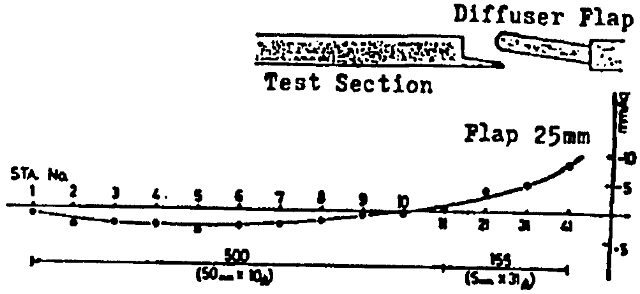

Figure 4. Static Pressure Distribution on the Wall of Measurement Part

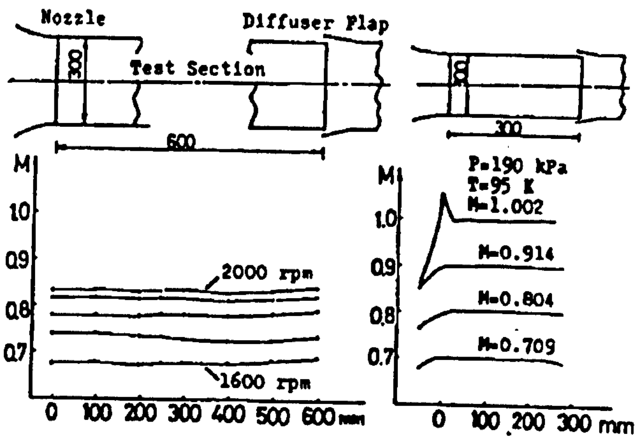

Figure 5. Mach Number Distribution on the Wall of Measurement Part

4. Conclusion

Replacement of the exhaust valve by an automatic valve has made it possible to control the internal pressure of a wind tunnel to arbitrarily set pressure in the allowable range of the internal pressure of the wind tunnel. One of the three control variables (temperature inside a wind tunnel, internal pressure on the wind tunnel, and air current velocity) has become controllable. Of the remaining two variables, the device is currently being revised for the temperature inside a wind tunnel, and the same is being planned for air current velocity (number of fan rotations).

If these variables become completely controllable, the air current allowing free selection of a Mach number and a Reynold's number in an extensive operation envelope diagram becomes realizable, with pressure, temperature, and wind velocity set arbitrarily. Figure 6 shows the calculated limits of the operation envelopes for this wind tunnel and those for the Aeronautical Technology Research Institute's wind tunnel. Since the size of measurement part differs in both wind tunnels, the above-mentioned limits are compared

on the assumption that $\bar{c} = 0.1\sqrt{A}$ (A: sectional area of the measurement part).

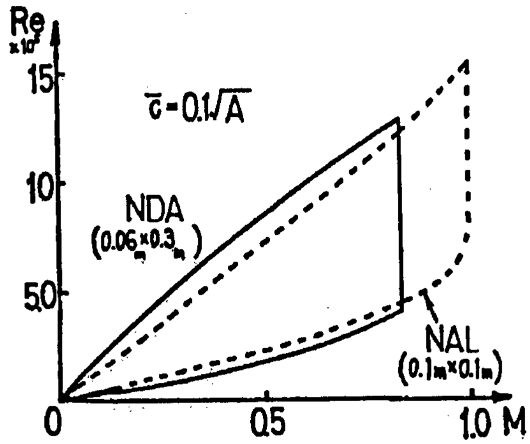

Figure 6. Operation Envelope Diagram

For the static pressure distribution and air current velocity distribution on the measurement-part wall surface, data was taken at more measurement points than those previously measured, and was compared with the previous data. However, no change was found in the general trend.

Advisor: Assistant Professor Yutaka Yamaguchi

BIBLIOGRAPHY

1. Kjlgore, R.A. and Dress, D.A., CRYOGENICS, September 1984.

2. Yoshizawa, JOURNAL OF JAPAN AERONAUTICS AND SPACE SOCIETY, No 351, Vol 3, April 1983.

3. Yamaguchi, et al., "Lecture Meeting of Western Branch of Japan Aeronautics and Space Society," 1985.

4. Yamaguchi, "17th Lecture Meeting of Japan Aeronautics and Space Society," 1986.

Optimum Spare Parts Arrangement

43062532a Tokyo BOEI GIJUTSU in Japanese Sep 87 pp 59-61

[Report by Atsushi Aizawa, student, Operational Research System Faculty, Defense Academy: "Optimum Arrangement of Spare Parts With Environmental Conditions Taken Into Consideration"]

[Text] 1. Preface

Since complex devices require high-level techniques for repair, they are not repaired in the field when they fail. Instead, failed parts are replaced for each unit and repairs collectively performed in a central maintenance factory.

In this case, not all the spare units are kept in the central maintenance factory due to the transport time involved, but some are kept in advance in each area as spare units to effectively enhance the working ratio.

In the Ground Self-Defense Force, for example, the above-mentioned work is performed by the central maintenance factory and individual local repair shops. However, since storing spare units is limited due to control of expenses, their optimum distribution becomes a problem.

In this problem, the number of devices needs to be thought of as comparatively large, the analysis method using a Markov's transition diagram is actually impossible and an approximate solution becomes indispensable. Actually, two-step supply systems are being studied using various approximate solution methods, but these studies are all being analyzed under the condition that the operating environments of the devices are the same. However, when the same device is used throughout Japan, as is done by the Ground Self Defense Force, environmental influences need to be taken into consideration since environmental changes depend on each operating area.

This report investigates optimum numbers (minimum numbers of spare units to keep the probability of spare part shortages in the field below fixed values) when environmental conditions differ depending on individual fields.

2. Assumptions

(1) At time 0, m identical units are being used in n areas and m_i units are operated in area i ($i = 1, 2, \ldots, n$).

(2) The units in each area are independently operated and the failure rate of each unit in area i is λ_i.

(3) Area i has S_i spare units at time 0.

(4) Only one maintenance factory is available and all failed units are repaired in this factory. The average repair time is $1/\mu_1$ ($m_1 \neq 0$) and

includes the transport time to and from the area, delay time, and inspection time after repair completion. A unit whose repair has been completed becomes a spare unit of the maintenance factory. At time 0, all the units are normal.

(5) The maintenance factory has S_D spare units at time 0.

(6) If a failure occurs in an area, the failed unit is immediately replaced by a new unit if a new unit is in the area, and the failed unit is transported to the maintenance factory. The replacement time is assumed to be negligible. Also, if a spare part is in the maintenance factory, it s transported to area i. The average transport time to area i is $1/\mu_{2i}$ ($\mu_{2i} \neq 0$). If an area has no spare unit, it waits for transport of a spare unit from or repair of the failed unit by the maintenance factory.

3. Symbols

λ : Average failure rate of all areas

$$\lambda = \sum_{i=1}^{n} \lambda_i \cdot m_i$$

R_i : $\lambda_i \cdot m_i / \lambda$

A_i : $\lambda_i \cdot m_i / \mu_{2i}$

P_i^* : Allowable lower limit values of the probability of no spare unit shortage occurring in each area.

S : Vector showing arrangement of spare units

$$S = (S_D, S_1, S_2, \cdots\cdots, S_n)$$

$P_i(S)$: Probability of no spare unit shortage occurring in area i when the number fo spare units in the maintenance factory and area i is S.

B : λ/μ_1

ℓ : Number of failed units in all the areas during time $1/\mu_1$

F : $\ell - S_D$

S_0 : $S_D + \sum_{i=1}^{n} S_i$

$\binom{n}{r}$: Combination of r items from n items

S_0^* : Optimum number of spare units

4. Analysis

(1) On the assumption that no spare unit shortage occurs in the maintenance factory, the necessary number of spare units S_i is determined for each area.

First the minimum S_i that satisfies the relationship

$$\exp(-A_i)\sum_{k=0}^{si}\frac{A_i^k}{K_i}\geq P_i^*$$

is obtained, and is assumed to be the necessary number of spare units for each area. The right side of this relationship is the probability of no spare unit shortage occurring during time $1/m_{2i}$ in area i when the assumption is made that no spare unit shortage occurs in the maintenance factory. Let this be P_i (∞, S_i, μ_{2i}).

(2) Suppose that the number of spare units in area i is S_i, the number of spare units in the maintenance factory is S_D, and the transport time from the maintenance factory to each area is 0. Then, the probability P_i S_D of no spare unit shortage occurring in area i during time $1/\mu_1$, while the average failure rate of all the areas and the average repair time of all the units are being taken into consideration, is obtained as shown below:

a. The probability $P(\ell)$ of ℓ units failing in all the areas during time $1/\mu_1$ is

$$P(\ell)=\frac{e^{-B}\cdot B^{\ell}}{\ell\,!}\quad(\ell=0,1,\cdots\cdots)$$

b. At this time, the probability $Pi\cdot S_D(\ell)$ of no unit shortage occurring in area i, when ℓ units failed in all the areas during time $1/\mu_1$, is obtained. Since, if the number of failures in area i is fewer than the number of spare units of the area (S_i), numbers of failures in other areas are insignificant, $Pi\cdot S_D(\ell)$ becomes as shown by the polynomial theorem.

$$P_i\cdot S_D(\ell)=\sum_{ki=0}^{S_i}\sum_{k1=r1}^{t1}\cdots\sum_{k(i-1)=(i-1)}^{t(i-1)}\sum_{k(i+1)=r(i+1)}^{t(i+1)}\cdots\sum_{k(n-1)=r(n-1)}^{t(n-1)}$$

$$\times f\,(F,k1,k2,\cdots\cdots,k(n-1))$$

$$(S_D\leq\ell)$$

$$f\,(k1,\cdots\cdots,k(n-1))=\begin{bmatrix}F\\k1\end{bmatrix}\cdots\cdots\cdots\begin{bmatrix}F-k1-\cdots\cdot-k(n-2)\\k(n-1)\end{bmatrix}$$

$$\times R_1^{k1}\cdot R_2^{k2}\cdots\cdots R_n^{F-k1-\cdots-k(n-1)}$$

$$rj=\max(0,F-ki-k1-\cdots\cdot-k(j-i)-(m(j+i)+S(j+1))-\cdots\cdots-(mn+Sn))$$

$$tj=\min(mj+Sj,F-k1\cdots\cdots\cdots k(j-1))$$

c. From a and b, the desired probability $P_i \cdot S_D$ is

$$P_{i \cdot SD} = \sum_{l=0}^{\infty} P(l) \cdot P_{i \cdot SD}(l)$$

(3) The minimum S_D which satisfies the relationship max $(P_i)^* \leq P_i \cdot S_D$ in all the areas is obtained (i = 1, 2, ...n, n).

(4) Let $P_i(S) = P_i\ (\infty, S_i, \mu_{2i}) \times P_i \cdot S_D$

(5) By changing S_D and S_i, the minimum number of spare units $S_0{}^*$ (the number of spare units in the maintenance factory + the number of spare units in individual areas) can be determined so that the spare unit shortage rate becomes equal to or less than $1-P_i{}^*$ (that is, $P_i(S) \geq P_i{}^*$) in each area.

6. Numerical example

The algorithm and numerical examples for determination of optimum numbers of spare units have been omitted due to a limitation on the number of pages.

Advisor: Professor Masabumi Sasaki

BIBLIOGRAPHY

1. Malec, Henry A. and Steinhorn, Daniel, "A New Technique for Depot and Subdepot Spares," IEEE TRANS., on R. Vol. R-29, 1980, pp 381-386.

2. O'Neil, F.J., "A Two-Level Sparing Approach for Plug-In Modules," IEEE, Proc. 1983 Annual R.& M. Symp., pp 388-393.

20111/9365

Reorganization of TRDI, Projects Discussed

Tokyo BOEI ANTENA in Japanese Oct 87 pp 51-62

[Text] Research and Development

Recently, the qualitative change in equipment has become marked with the advance of science and technology. The equipment has become complex, and its performance has increased. Accordingly, this change has brought about a revolution in military strategies and tactics. Foreign countries are making every effort to modernize equipment, and in particular, the free world countries are conducting R&D on equipment to which high technology is applied.

It is necessary for Japan to qualitatively increase and enhance defense power so that the technical level can correspond to that of foreign countries. In order to do so, it is important to work to complete the technical R&D posture. The Defense Agency has the TRDI (Technical Research and Development Institute) which conducts R&D of equipment for three services, the GSDF (Ground Self-Defense Force), the MSDF (Maritime Self-Defense Force), and the ASDF (Air Self-Defense Force). The TRDI conducts R&D on various equipment such as aircraft, missiles, combat vehicles, electronic equipment, by fully utilizing excellent Japanese technologies.

Japan herself conducts R&D on equipment necessary for her defense. This means that she has the following advantages: 1) she can have equipment specifically suited to the country; 2) it will become easy to maintain and supply equipment over a long period of time; and 3) she can maintain and increase the technical foundation for equipment production.

2. Main Research and Development Items

(1) New tank

A new tank is being developed to succeed the operational Type-74 tank. It is armed with a 120-mm tank gun, and has excellent mobility and armor. It can attack the enemy by using this tank gun at night while the tank is moving.

(1) Surface-to-ship guided missile

The surface-to-ship guided missile can be launched from inland areas; it is the first time the XSSM-1 system is used in Japan. It is controlled with a composite guidance system consisting of an inertial guidance system and an active wave homing system, and is used to defeat enemy ship assault forces off-coast. Its development work will be completed in this fiscal year.

(3) Intermediate class trainer.

The intermediate class trainer T-4 aircraft succeeds the jet trainer T-33 used to train ASDF's recruit pilots. This jet trainer's development, including the engine, is being conducted domestically. At present, the flight tests are progressing smoothly, and the development work will be completed in this fiscal year.

3. Reorganization of Research and Development System

In recent years, TRDI's R&D has become increasingly advanced and complex. It is anticipated that the amount of this work will increase. In consideration of this situation, TRDI has completed its research sections for the following items by reducing the scale of research on food, clothing, etc., since FY 1987: 1) Items which have high secrecy or cannot easily be obtained, for example, command and communication, equipment for electronic warfare, etc.; and 2) items in which the government cannot avoid taking the lead, because there is no demand for these items in private companies, for example, firearms, ammunition, etc. It is believed that the R&D posture will be built up to flexibly correspond to R&D work which will be required by three services.

4. Modernization of TRDI

The scale of this TRDI modernization is the greatest since the 1958 modernization.

The system and research items of TRDI are as shown in the "FY 1986 TRDI Organization Chart."

The TRDI has been reviewing the R&D system since March 1984 because of a demand for administrative reform by the "Urgent Enforcement Policy Concerning Administrative Reform" decided upon by the Cabinet on 25 January 1984. As a result, it has been decided that system modernization will be required in FY 1987 and will be enforced on 1 July [1987]. This modernization covers not only the reform of the system mechanism, but also the review of a series of R&D activities extending from establishment of R&D goals, to evaluation of results. In addition, the modernization covers a comprehensive radical reform including the use of private companies and tie-ups with relevant organizations.

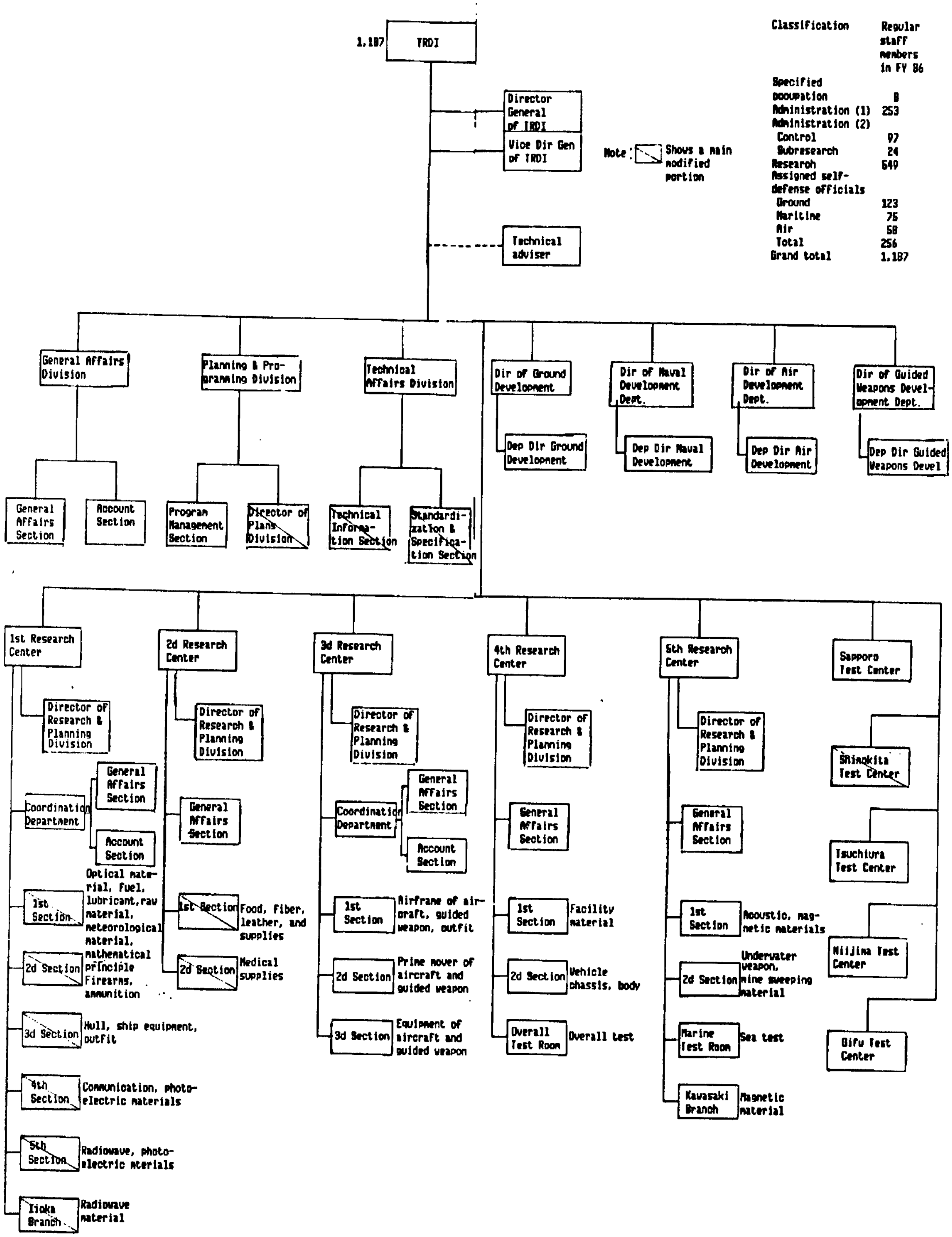

Organizational Chart of TRDI in FY 1986

Progress of TRDI's Budget for Defense-Related Expenditures

Classification	1983	1984	1985	1986	1987
Defense-related expenditures (A)	27,542	29,346	31,371	33,435	35,174
(Percent) growth from previous fiscal year	6.5	6.55	6.9	6.58	5.2
TRDI's budget (B)	386	438	578	653	733
(Percent) growth from previous fiscal year	8.4	13.3	32.1	12.9	12.3
B/A (percent)	1.40	1.49	1.84	1.95	2.08

(Unit: ¥100 million)

The main modernization contents are as shown below:

(1) Modernization of Planning & Programming Division and Technical Affairs Division

a. The Planning and Programming Division has been modernized so that it can handle work such as priority R&D, use of technical power of private companies, promotion of project team systems, and exchange of technical information.

b. The investigation and analysis functions have been completed by evaluating the technical information on R&D which has been carried out up to now and by evaluating the technical level necessary for reinforcing the system. As a result, the Technical Information Section of the Technical Affairs Division has been abolished, and the No 1 Technical Section has been established.

c. The Standardization & Specification Section of the Technical Affairs Division has been abolished, and the No 2 Technical Section has been established. This new section covers the work of patent, data, and library which were under the charge of the Technical Information Section and the work of standardized specifications, etc., which were under the charge of the Standardization & Specification Section in order to consolidate control of the R&D result.

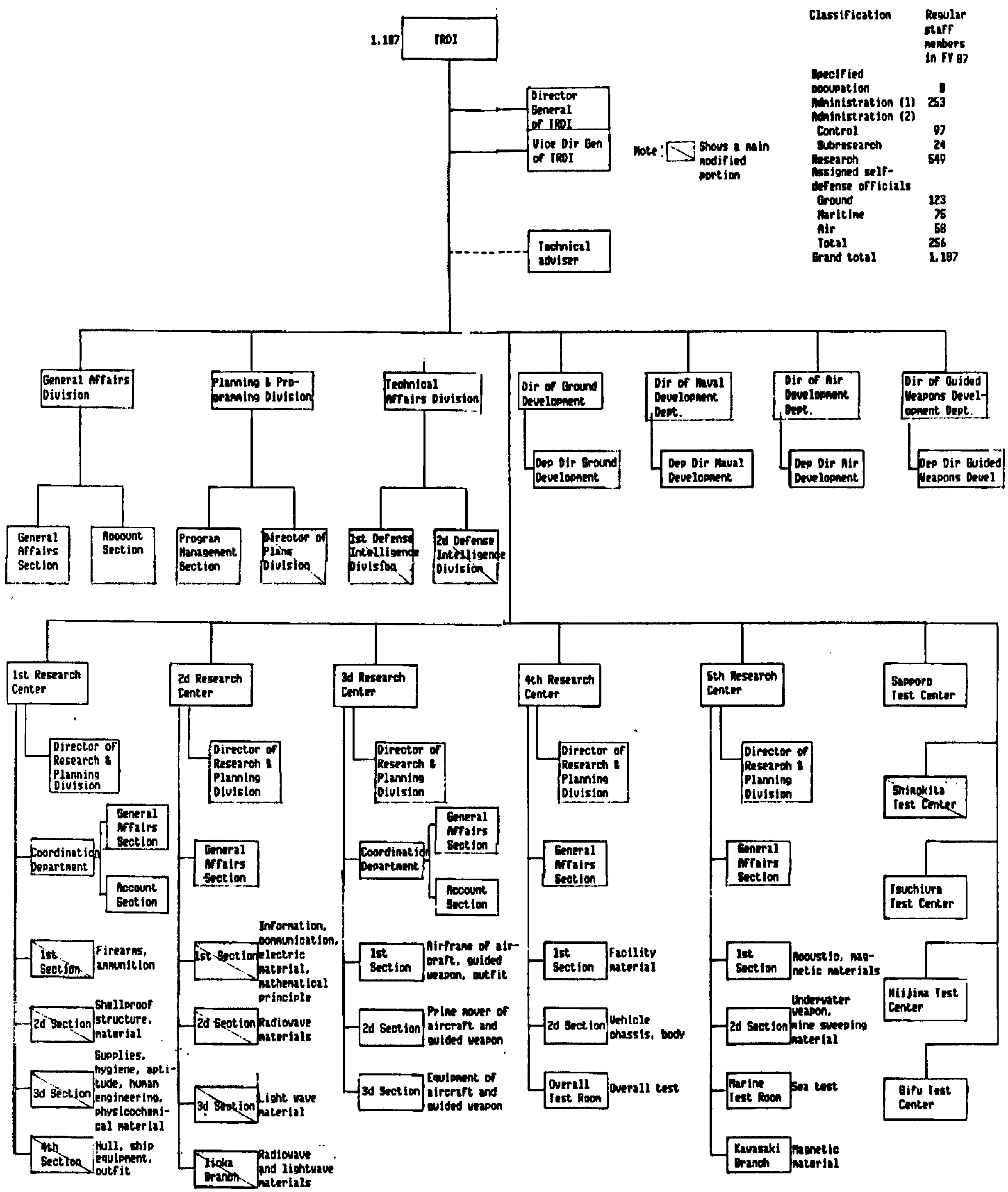

Organizational Chart of TRDI in FY 1987

(2) Modernization of Research Centers

a. 1st Research Center

The 1st Division is in charge of firearm and ammunition, and the 2d Division is in charge of shellproof structures. Research rooms are under their respective technical elements, and a system research room intensively integrates these research rooms. It has been decided that the 1st Division will be completed and built up so that this division can meet the needs of the times.

The 3d Division as a protective and lifesaving division is in charge of food, clothing, health and welfare, which were under the charge of the obsolete 2d Research Center, and is in charge of the fuel,lubricant, etc., which were under the charge of the 1st Division of the obsolete 1st Research Center. Also, human engineering matters have gained importance as items in the 3d Division.

It has been decided that the optical and electronic matters-related section of the 4th and 5th Divisions of the obsolete 1st Research Center will be established as the 2d Research Center and will be separated from other divisions; the 4th Division will be newly integrated as a ship section into research rooms necessary for matters related to defense problems such as new materials, noise abatement, etc.

b. 2d Research Center

The 4th and 5th Divisions of the original 1st Research Center and Iioka Branch have been modernized so that they can be in charge of the optical and electronic matters such as C^3I (command, control, communications, and intelligence), radar equipment for electronic warfare, laser equipment, infrared rays, etc., whose technical innovation is remarkable.

The 1st, 2d, and 3d Divisions are in charge of information and communication, radiowaves, and lightwaves, respectively; each division consists of research rooms in charge of each technical element, and a system research room which controls these research rooms. Also, a computer room was in the 1st Division of the 1st Research Center up to now, but has been installed as a computer center in the 1st Division of the 2d Research Center.

c. Other Research Centers

The name of research rooms has been changed so that each name is suitable for actual situations of each work, and a new research room has been established in the 3d Division of the 3d Research Center. This new research room will be in charge of technologies for integrating electronic equipment which will be installed in aircraft.

(3) Modernization of Test Division

A new test planning section and a new test section have been established in the test team of the Shimokita Test Center for the purpose of enhancing the evaluation of tests on firearms and ammunition.

PRODUCT, APPLICATIONS OF OXYGEN FREE METAL BALL POWDER DISCUSSED

43067502 Tokyo KINO ZAIRYO in Japanese Sep 87 pp 37-42

[Article by Kenzo Kamon, chairman, Toyo Metal Co., Ltd.: "Oxygen-Free Production of the Powder of Perfectly Round Metal Globules and Its Applications"]

[Excerpts] By applying metal melting experiments in space, oxygen-free production of the powder of perfectly round metal globules was successfully carried out. Because of production in the oxygen-free state, metal characteristics are given full play. Since perfectly round globules are obtained, the powder excels in fluidity which makes it highly useful for applications in such fields as paint and ink. In this paper, special production in the oxygen-free state of the powder of perfectly round metal globules is summarized, together with an explanation of its applications.

1. Metal Powdering Processes

There are some forty or fifty types of metal powdering processes. Use of a specific process is determined by purpose and the type of metal used.

Some typical processes currently in use are shown below:

(1) Mechanical Milling Processes

1) Stamping process - Powdering metal in a way rice cake is made.

2) Ball milling process

(1) Dry type - While a cylindrical tank is turning around, balls are placed inside the tank for powdering.

(2) Wet type - Stearic acid used for materials subject to explosion and other hazards is placed and the wet type powdering is performed.

3) Other processes using rotary blades

(2) Physical Powdering Processes

1) Atomizing process - Molten metal is poured through a nozzle and sprayed by water, oil, inert gas, etc. for powdering.

2) Rotary electrode process - A molten mass is melted by using an electrode, and scattered by the centrifugal force.

3) Rotary disk process - A rotary disk is turning around at high speed directly under the nozzle, and molten metal is scattered by the centrifugal force.

4) Rolling process - Molten metal is rolled into foils or a metal mass is rolled into powder.

5) Dropping into water process - This method literally drops molten metal into water. Used for large drops such as shotgun pellets.

6) Molten metal rabbling process - Molten metal is rabbled immediately before solidification for powdering.

(3) Chemical Processes

1) Electrolysis process - Powder is produced by electrolytic deposition of the aqueous solution of metallic salt.

2) Evaporation coagulation process - A metal is heated for evaporation, and the evaporated metal is coagulated and recovered.

3) Extraction process - A metallic solution is subjected to reaction with a chemical and a metal is extracted.

Metal powder consists of different materials, shape, and grade depending on intended usage and its manufacturing process is diverse--from shotgun pellets and bearings for the powder of large metallic globules to welding, metallizing, circuit printing of electronic substrates for the powder of globulites. When it comes to the powder of globulites, it is used for paint, printing, ink, and coloring materials. Its applications cover a very wide field. As more uses are developed, metal powder is expected to develop considerably as a growth industry.

Recent years have seen new techniques developed in such a way that there is renewed interest in the characteristics of the powder materials. Advances in application techniques and processing techniques have contributed to expanding the scope of the usage of metal powder. Every manufacturer in this line is hard at work developing its usage from space rockets, aircraft to automotive parts or electrical and electronic parts.

2. Oxygen-Free Production of the Powder of Perfectly Round Metal Globules

The greatest problem of powder which is its advantage as well as its disadvantage is that the finer a globule is subdivided the larger its surface area becomes. Oxidation of the metal surface proceeds as much as the degree of surface area expansion. It is no exaggeration to say that metal defects begin with oxidation. To minimize this process of oxidation, the most desirable process is to manufacture globules in the oxygen-free condition. And the perfectly round globule provides a minimum of surface area. The

oxygen-free powder of perfectly round globules is considered to be the material that can give full play to its materials characteristics peculiar to metal. It is well known that metal dissolution tests in space have been conducted in the space shuttle, creating a great sensation in the metal materials industry. In this paper, a process of manufacturing the oxygen-free powder of perfectly round globules using this space principle will be introduced (see Figure 1 Manufacturing Process).

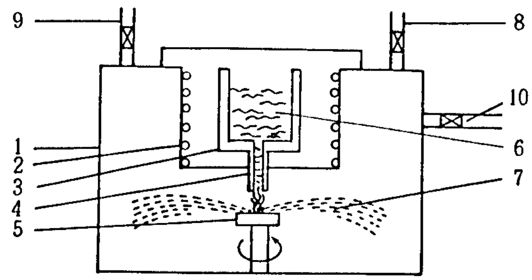

図2

1)	真空タンク	真空度は10^{-3}に耐えうる構造
2)	ヒーター	製造する材料の融点で選定
3)	ルツボ	製造する金属材料にて異なる
4)	ノズル	同　上
5)	回転ディスク	形状は金属の性状により平形，山形，凹形を選定する
6)	溶湯	金属の融点より＋50度以上が好ましい
7)	粉末	遠心力により飛散した金属粉体
8)	ガス入口	He, N_2, Ar, H_2, CO_2 等
9)	ガス出口	同　上
10)	真空パイプ	

Figure 2

Keys:

(1)	Vacuum tank	Structured to withstand a degree of vacuum of 10^{-3}.
(2)	Heater	Selected in terms of the melting point of a material to be manufactured.
(3)	Crucible	Depends on a metal material to be made.
(4)	Nozzle	Same as above.
(5)	Rotary disk	The shape is selected out of the horizontal, peak, and concave types according to the metal properties.
(6)	Molten metal	Preferably at least 50 degrees CC more than the melting point of the metal.
(7)	Powder	Metal powder sprayed by centrifugal force.
(8)	Gas inlet	He, N_2, Ar, H_2, CO_2, etc.
(9)	Gas outlet	Same as above.
(10)	Vacuum pipe	

2.1 Rotary Disk Process

There are several types of the processes of making powder in the oxygen-free state of perfectly round metal globules. The rotary disk process will be explained here. Figure 2 shows the basics of the rotary disk process.

The manufacturing procedures of the powder in the oxygen-free state of perfectly round metal globules is explained in Figure 2. First, vessel 1 is subjected to evacuation to a degree of vacuum in excess of 10^{-3}; then, it is filled with a high-purity inert gas. This inert gas should always be more on the plus side than the atmospheric pressure, and during operation, the gas must be poured continuously to eliminate cooling heat as molten metal in high temperature is cooled and powdered. An explanation, at this point, of what makes perfectly round globules will aid understanding:

In Figure 2, molten steel 6 in crucible 3 which has been heated by heater 2 drops onto disk 5 in tank 1. Since the disk is turning at 10,000 - 40,000 revolutions, its centrifugal force sprays molten metal and powder as shown in 7. Molten steel thus sprayed solidifies before reaching the drop point. Just like melting metals in space, metal which has been cooled and sprayed condenses in the gravity-free state so that a resultant surface tension causes the globules to be perfectly round. Conditions should be determined by taking into full consideration the characteristics of each metal.

A few cases of different metals will be explained below.

2.2 On the Hemicrystalline Solder

The hemicrystalline solder is composed of Sn 61.9 percent and Pb 38.1 percent with a hemicrystalline temperature of 183 degrees C. Maintain this material at high temperatures from 50 degrees C to 100 degrees C and drop the molten metal through the nozzle tip. Then, the rotating disk sprays and powder it. To make perfectly round globules at this time, oxygen in the vessel must be minimized so that it is necessary to evacuate the vessel to a degree of vacuum in excess of 10^{-3}.

2.3 Adjusting the Globule Size

Since adjusting the globule size varies with each type of metal, it must be determined through building up test data. Conditions are determined by (1) molten metal temperature, (2) inner diameter of the nozzle, (3) revolving speed of the disk, and (4) shape and materials of the disk. By adjusting these four factors, any globule size can be obtained. In this rotary disk process, about 70 percent of the globules have a size from 45μ to 150μ.

2.4 Zinc Powder

Zinc's melting temperature is 419.4 degrees C. Therefore, the optimum furnace temperature for powdering is 450 degrees C - 500 degrees C. When dropping Zn, attention should be paid to the nozzle so that it will not be clogged during the process of cooling with molten Zn solidifying. If the nozzle becomes clogged, it must be heated. The globule size is the same as the above-

mentioned solder. Since the temperature is higher than solder, care is required.

2.5 Aluminum Powder

The higher the purity of aluminum is, the more difficult its powdering is. Powdering of alloy materials is relatively easy. Its smaller specific gravity than that of solder and zinc seems to be partial cause of the powdering difficulty. With aluminum, special attention should be paid to the material and shape of the disk. Currently, there is no conclusive evidence to recommend any specific material or shape.

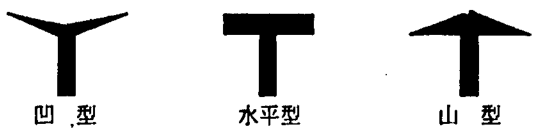

図3

Figure 3

Concave type Horizontal type Peak type

2.6 Rotary Disk

It is no exaggeration to say that the disk is the key to making the powder in the oxygen-free state of perfectly round globules. The function of the top of the disk 5 in Figure 2 is to receive molten metal as it falls or drops and to spray it by centrifugal force. The manner in which it is sprayed determines the shape and size of globules for powdering. Consequently, the shape and materials of the disk is the determining factor of the powder to be recovered.

Disk shape can be roughly divided into three types as shown in Figure 3. The concave type is suited for the powder of small globule size, the peak type for the powder of relatively large globule size, and the horizontal type for the powder of intermediate globule size. This classification should not be applied for all purposes. Depending on the type of metal such as the one with light or heavy specific gravity, the shape and angle should be changed.

Disks are made of iron, stainless steel, graphite high-speed tool steel, tungsten carbide, zirconium, ceramics, titanium, silicon nitride, aluminum, etc. The most critical factor is that the metal be wettable. The reason why wettability varies so much with the type of metal arouses scientific curiosity. Another requirement is that the disk material be able to withstand long hours of operation. Wettability is required because when the disk is turning around at high speed while producing centrifugal force, a metal piece that falls down remains on top of the disk in the neck-shaking state and breaks while drawing a large circle. Wetting enables it to shake off the metal piece dropped to the disk top to prevent the metal piece from solidifying and sticking. Although the angles of concavity and peak need not be too large, some adjustment is required to determine the globule size. The proper diameter of a dish on the disk is from 20-mm - 40-mm. Also, because this diameter is related to the size of globules in the powder, experimental

tests should be repeated to gather data with which to establish the manufacturing conditions.

When molten metal drops onto the dish on the disk, if the disk is cold, it will stick to the dish and will not spray. Hence, an essential process is that before the molten metal drops, the disk be heated close to the melting temperature of the metal to be powdered so that the molten metal drops can be sprayed at the disk surface by the wetting and centrifugal force.

The foregoing explanation has covered the main points and problems in the oxygen-free production of the powder of perfectly round globules.

3. Application of the Oxygen-Free Powder of Perfectly Round Globules

In recent years, metal powders have been used in virtually every field. Their materials are metals that come to our attention in our daily life such as iron, copper, aluminum, magnesium, zinc, lead, gold, and silver. They are the metal elements existing on the earth which are used as single elements or alloys of many shapes. For example, their use includes warm pocket heaters at home, ceramic pots and pans, paint for home decorating and sintered machinery parts. They are also used widely for a variety of industrial materials. As advances in the powdering process and processing techniques are made in the future through technological development, their scope of usage is expected to expand.

3.1 Classification by Usage

1) High technology - High-temperature powders for space rockets, aircraft, etc.

2) Machinery materials - Sintered parts and abrasion-resistant materials

3) Electrical parts - Magnetic materials, conductive materials, and electric heating materials

4) Building materials - Exterior, interior, decoration, and sintered metal tiles

5) Resin fortified materials - Mixed in resins as fortifier

6) Resin conductive materials - Mixed in resins as conductive material

7) Decorations - Gold, silver, and other accessories and decorations

8) Arts and crafts - Buddhist altars, Buddha statues, ornaments, sculptures, and chinaware

9) Textile products - Antistatic, carbon fiber

10) Optical instruments - Coating through metal vapor deposition

11) Testers - Sensors and circuit parts

12) Vehicle parts - Engine components, braking devices

13) Welding materials - Brazing filler metals and anti-abrasion materials

14) Metallizing materials - Metal powder metallizing materials

15) Kitchen items - pots and pans, and tiles

16) Paint - Silver pen anticorrosive paint and metallic paint

17) Ink - Printing ink, pigments, and dyes

18) Colors - High-grade coloring materials for mural paintings of ancient China, etc.

19) Others - Filter bearings and other materials

As presented above, the usage of metal powders is extended to all sectors of industry and every field of our life. The manufacturing process and processing methods vary depending on use. The powder of perfectly round globules of the oxygen-free metal is explained in detail below:

3.2 Advantages of Oxygen-Free Production

Because globules are manufactured in the oxygen-free state, the material quality is extremely pure. Consequently, the metal characteristics are given full play. With no danger of defects due to materials, these globules has high reliability and are especially effective in the production of electronic or other products requiring high-level technology.

3.3 Advantages of Perfectly Round Globules

1) Compared with many other types of particles, the surface area is minimum so that the progress of oxidation due to manufacturing and processing can be held to a minimum.

2) Since the perfectly round globules have good fluidity, during processing or supplying materials, they can be supplied very smoothly without clogging. Therefore, their effectiveness comes into full play when supplying the fixed amounts mechanically by using dispensers, etc.

3) When using them for paint, globulites are needed. No uneven painting occurs in painting with brush. Also, because they are mixed in organic materials, uneven mixing due to a difference in specific gravity is prevented.

4) When using them for printing ink or pigments, submicron particles are required. Since they are globulites, uneven mixing is prevented and a beautiful finish is obtained.

5) In the case of screen printing of circuits for electronic substrates, their fluidity is so good that no printing errors occur. Their exceptional

reliability is such that there are no better materials than the oxygen-free powder of perfectly round globules.

6) In using them as blast-grinding material, because the globular face hits the workpiece, luster griding is performed to provide a fine finish.

The above explanation has covered, in general, the advantages of the oxygen-free production as well as the advantages of perfectly round globules. It is expected that as continuing efforts are made to take advantage of both merits, their scope of applications will expand more and more. The powder of perfectly round globules of oxygen-free metals has caught industry-wide attention and every manufacturer is conducting research and development of new products.

Next, we will discuss a few examples of new products under development:

4. Development of New Alloy Materials

Superconductive materials whose research and development is made on a worldwide basis is well-known. In due course, materials, which generate a superconductive phenomenon in near room temperature, and processes of generating such phenomenon will be developed. Whether of metal or ceramics, these materials will probably be powdered to processing into serviceable materials. Since the discussion has jumped to high technology, let me point out that development of new alloy materials is being pursued with the assumption of new powder methods.

(1) Heat-resistant materials

Manufacturers are hard at work developing heat-resistant materials with higher efficiency mainly for space and aeronautical applications.

(2) Abrasion-resistant materials

Much work is underway to develop metal oxides, which are also being developed as abrasion-resistant or heat=resistant materials.

(3) Electronic substrate materials

Metals of relatively low melting points are used. The powder of perfectly round submicron globulites currently in need is to be developed in the future.

5. Development of Powder Processing Methods

The foregoing discussion has covered the manufacturing processes of metal powders. By powder processing methods is meant methods of obtaining characteristics unobtainable with the conventional metal processing methods by changing the composition of metal materials or atomic orientation. It is known that amorphous materials having characteristics different from their own composition can be made. Powders, depending on their processing methods, can obtain different characteristics. The oxygen-free powder of perfectly round globules is a case in point, as explained in detail above.

5.1 Powder Forging Method

A metal powder is sintered or other metals are added to it. Then it is subjected to die forming or its component material is subjected to forging forming to produce a material having different characteristics from the conventional material.

5.2 Powder Extrusion Method

A single substance or a large quantity of alloy materials is added to a powder to obtain an ultrafine structure, thereby greatly improving the characteristics of the powder. Also, development of new materials is being conducted by adding different metal ceramic, etc.

5.3 Chilling Solidification Method

The characteristics of solidification through chilling are, in addition to the above-mentioned amorphous characteristics: (1) expansion of the solid solution limit of alloy elements, (2) making grains ultrafine, and (3) making alloy components uniform. As a technique for further development of new materials, many expectations are entertained for this method.

6. Conclusion

The manufacturing process and applications of the powder in the oxygen-free state of perfectly round metal globules have been explained from a general standpoint. The reader should understand that many powders are used in products we use without noticing in our daily life.

The manufacturing process and the device for the rotary disk process as explained in this paper are patented.

/12913

Current Status of Optical Communications Discussed

Subscriber-Based Optical Communications

43066518 Tokyo OPTRONICS in Japanese Nov 87 pp 82-88

[Article by Teiji Shimada and Koichi Sano, NTT: "The Current Status and Future Trend of the Subscriber-Based Optical Communications System in Japan"]

[Excerpt] 1. Preface

The subscriber-based optical communications system comprises optical fiber transmission technology, exchange technology, multiple-separation technology, LSI technology, network operation technology and interface standardization, thereby covering a wide range of fields. Therefore, it is natural that a more systematic approach be necessary to develop the optical communications system.

The authors would like to discuss the current status of the subscriber-based optical communications system and its future trends in Japan.

2. Current Status of Subscriber-Based Optical Communications System

Around 1977, research involving elemental technologies, such as WDM transmission technology, started triggering the substantial research and development of Japan's subscriber-based optical transmission system around 1980. Table 1 presents the brief history of the research and development status of the subscriber-based optical communications system in Japan.

As clearly indicated from the trends, the connection with the CATV (community antenna television system) is extremely important in building up the subscriber-based optical system. However, from the standpoint of commercial application, the coaxial cable-based transmission system still prevails in terms of economy. As a result, with the exception of Hi-OVIS, the introduction of commercial optical transmission systems to CATV are limited to the very few cases in which they are applied as

Table 1. Brief Record of Research and Development for Subscriber-Based Optical Communications System

Name of System and Number of Subscribers		Name of Organization	Site	Services Offered	Operation Period
Hi-OVIS	168	Living Image Information Society	Higashi-Ikoma, Nara	C-E video, subscriber's line 1 Km "To offer a two-way video information system"	1978
Wire Hanamaki Television	2500	Wire Hanamaki Television	Hanamaki-city Iwate prefecture	C-E video, center facilities 2.5 Km "To improve the video quality"	1978
Lake City Cable Television	2700	Lake City Cable Television	Suwa-city, Nagano prefecture	C-E video, trunk line 14 Km "To carry out counter measures against electric wave problems"	1979
Yokosuka area subscriber-based optical communications system (field test)		NTT	Yokosuka city	C-E video high speed digital	1980
Wasoku-cho CATV	1500	Wasoku-cho CATV	Wasoku-cho, Kyoto	C-E videc, center facilities 8 Km "To protect from thunder hazards"	1981
Wide band optical private line system (field test)	4	NTT	Kichijoji, Tokyo	E-E video	1983
Dark area in optic communication system (on-site test)	27	NTT	Kichijoji, Tokyo	C-E image	1983
INS Model System (field test)	280	NTT	Mitaka city, Tokyo	E-E video, C-E video high speed digital, 64 Kb/s-based	1985
Combined subscriber-optical transmission system (field test)	30	NTT	Marunouchi, Tokyo	C-E video 64 Kb/s-based	1986
IBIS	200	MITI	Funaba, Osaka	C-E video (Advanced Hi-OVIS) digital 143 Mb/s	1986 ~

electric wave and thunder-induced hazard protection practices for CATV main trunk line systems (the transmission channel which connects the antenna installed on a hill and the head end in CATV or interconnects the CATV facilities is called the "main trunk line").

On the other hand, targeting the construction of the advanced information network system (INS), NTT tried to technologically confirm a subscriber-based optical and large-scale communications system which would make it possible to supply varied services in the future. NTT started the construction of an INS model system in 1984, completing it in 1987, which covered the Mitaka and Kasumigaseki areas. Figure 1 illustrates the basic construction of the subscriber-based optical communications system designed for the INS model system. Table 2 shows the main elements for the transmission system. This system adopts a single optical fiber in an effort to share the facilities of the subscriber's line so that several services, covering fields ranging from the 64 Kb/s system to wide-band communications systems, may be provided simultaneously based on the multiple wavelength. This system is also designed with specific attention paid to the module-based optical transmission unit, thereby enhancing the general purpose service.

In addition, NTT carried out an on-site test for the subscriber-based complex transmission system in the Marunouchi, Tokyo area, starting in 1986 and ending in 1987. This system was especially designed for the construction of commercially-oriented communications systems in order to accelerate the increase in demand for subscriber-based communications system, aiming at the establishment of thoroughly economical communications systems, which have been narrowed down to the interactive video distribution service and the 64 Kb/s system-based service. The mode parameters for this system are as follows:

(1) This system is mainly intended for the subscribers in large cities, setting 2 km as the transmission distance.

(2) This system adopts the LED (light emitting diode) as a light emitting element, since it is much lower in cost than the LD (lighting director), and selects the GI-type multimode optical fiber, paying specific attention to the coupling efficiency with LED.

(3) This system adopts multiple wavelengths, with consideration given to the current cost effect, and sets three different levels of wavelengths for the service, i.e., 0.78 μm, 0.88 μm, and 1.3 μm, respectively, with attention paid to the optical output of LED and its reliability.

(4) This system adopts an analog base band modulation system with consideration given to the frequency property and the economic efficiency of the LED, resulting in the installation of a subscriber-based video selection circuit to the center.

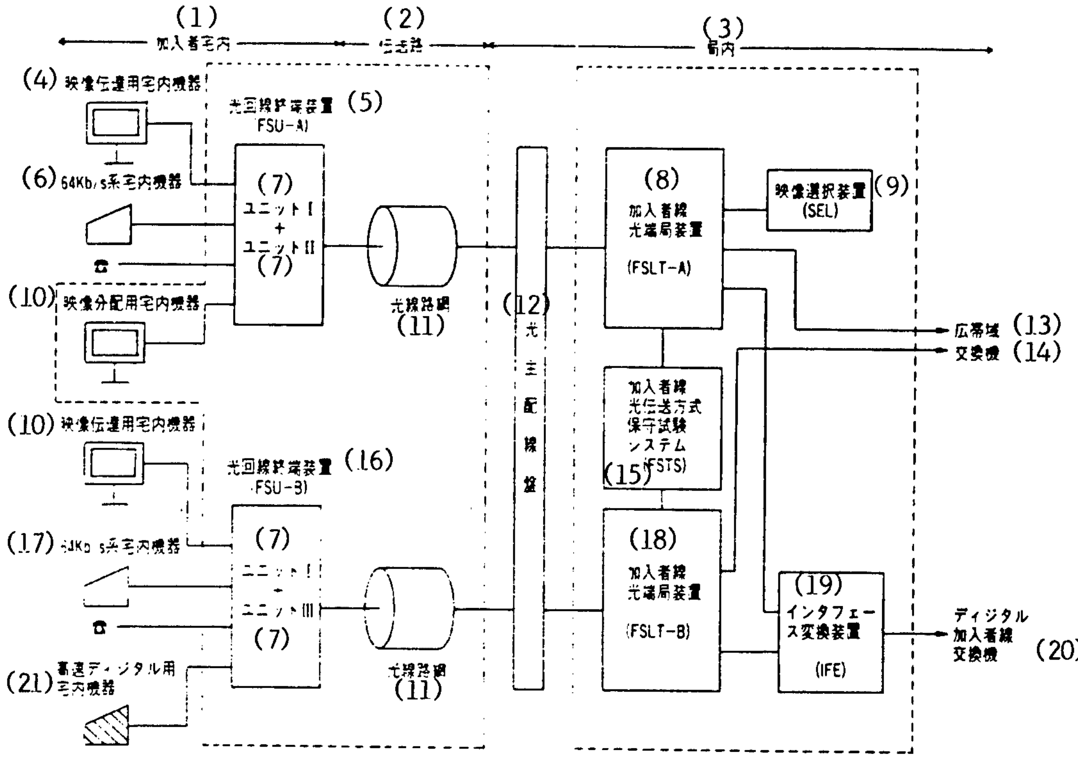

Figure 1. Basic Construction of Subscriber-Based Communications System in Japan

Key:

1. Subscriber
2. Transmission line
3. Station
4. Subscriber's equipment for video transmission
5. Optical line's terminal (FSU-A)
6. 64 Kb/subscriber's equipment
7. Unit
8. Subscriber's line optical terminal equipment (FSLT-A)
9. Video selection unit (SEL)
10. Subscriber's equipment for video distribution
11. Optical line network
12. Optical main distributing board
13. Wideband area
14. Exchange
15. Subscriber's line optical transmission system maintenance test system (FSTS)
16. Optical circuit terminating equipment (FSU-B)
17. 64 Kb/s-based subscriber's equipment
18. Subscriber's line optical terminal equipment (FSLT-B)
19. Interface converter (IFE)
20. Digital subscriber's line exchange
21. Subscriber's equipment for high speed digital

Table 2. Elements for Subscriber-Based Optical Transmission System in INS Model

Item \ Unit	Unit 1 (Basic Unit)		Unit 2 (Additional Unit)	Unit 3 (Additional Unit)	
Application service	• 64 Kb/s system video • transmission		• video distribution	• high speed facsimile • color facsimile	
Main transmission information	• 64 Kb/s system • video 1 ch (4.2 MHz, dual direction)		• video 1 ch (4.2 MHz, one-way)	• high speed digital 2 ch (0.77/1.5 Mb/s one-way)	
Application distance	5 km				
Wavelength in use	incoming 1.3 μm	outgoing 1.2 μm	outgoing 0.89 μm	incoming 0.81 μm	outgoing 0.89 μm
Illuminant	LD				
Multiplex wavelength	Maximum 4 multiplex wavelength (note)				

(Note) Unit I plus Unit II combination of Unit I plus Unit III is possible.

Table 3 shows the main system elements, Figure 2 [omitted] shows the system construction, and Table 4 indicates the main elements for the transmission system.

As discussed above, there are very few optical fiber communications systems available for commercial service in Japan. Furthermore, it is practically impossible to define them as full-fledged subscriber-based optical communications systems. This is due to the attention placed on the technological establishment of system functions and quality, with insufficient effort reserved for reducing the system cost, resulting in an imbalance between the cost and the service to be supplied. Therefore, the authors believe that more effort should be exerted to reduce the system cost when introducing full-fledged subscriber-based optical communications systems in the future.

3. Future Trends of Subscriber-Based Optical Systems

Table 5 shows a few typical subscriber-based optical systems which have been proposed for current study in Japan.

When predicting the technological and system trends of the future, it is thought that the single-mode optical fiber digital transmission method will predominate the subscriber-based optical communications systems. The single-mode optical fiber digital transmission method is currently more expensive than the existing multimode optical fiber analog-based band transmission method. However, it is expected that the introduction of LSI and OEIC/OOIC technologies will enable a dramatic reduction of adjustment sections and examination and test items to occur, as well as the transmission of a variety of unified information, including an image to exploit the wideband capacity of the optical fiber, thereby producing more profound economization than the analog transmission method. At the same time, the higher speed technology will progress year by year.

From the standpoint of forming the subscriber's network, a proposal has been made to improve the economic efficiency under the assumption that this single-mode optical fiber digital transmission technology will make steady progress together with the improvement in high speed performance. However, this proposal may be subject to some limitations in terms of system cost, if the connection between the center and the subscribers retains the traditional simple star network construction, although the cost of optical fiber may be reduced in the future. Therefore, a new approach to the problem is called for. More specifically, the introduction of the bus/star network construction will make it possible to share the center facilities and the subscriber's line, thereby attaining the total reduction. The authors would like to introduce a few examples of the subscriber-based optical communications system studied from this standpoint:

Table 3. Main Elements for Subscriber-Based Combined Optical Transmission System

Item	Contents
Service Functions	• One-way selection distribution (simultaneous 2 ch) of image (plus sound) • Optional connections (CUG, ID connection, toll confirmed connection) • Setting of dual-direction low-speed data channel (used for TV shopping, video retrieval service) • Access to 64 Kb/s INS network
Network Topology	Tree-type (trunk line system) + star-type (subscriber system) 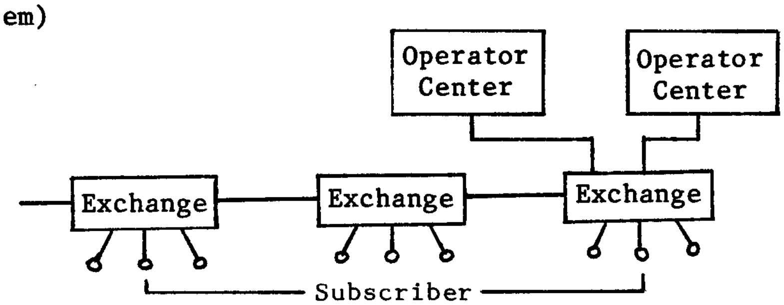
Transmission Quality	Image SNR: 43 dB (estimated value, 4.2 MHz)
Number of Channel Selectors	60 ch (10 ch are generally used for operation guide service)
Number of Operator Connections	8 max
Power Supply Mode to Optical Circuit Supply	Local power supply method based on commercial power supply

Table 4. Subscriber-Based Combined Optical Transmission System Elements

	Downward 1st Channel	Downward 2d Channel	Upward Channel
Transmission Signal	• image + sound • image-based control signal • low speed data • 64 Kb/s-based signal	• image + sound	• image-based control signal • low speed data • 64 Kb/s-based signal
Modulation	Analog base band-direct IM modulation		PCM-IM modulation
Luminous/ Light Reception Element	LED/APD	LED/APD	LED/APD
Service Wavelength	0.88 μm	0.78 μm	1.3 μm
Fiber	GI (50/125 μm)		
Transmission Distance	2 km		

Table 5. Main Examples of Subscriber-Based Optical Communications Systems Proposed for Study in Japan

Proposed System	Organization	Topology	Article
Digital optical CATV in bus/star type network construction	Fujitsu	Bus/star	CATV
Wideband optical subscriber network in double star network construction	NTT	Double star	CATV + E - E downward: TDM upward: TDMA
Subscriber-based optical communications network in multi-lane ring-type network construction	NTT	Ring star	To comply with the future service demanding vast volume and varied performance
Coherent optical FDM distribution-type subscriber-based communications system	NTT	Tristar	Experiment: 450 Mb/s 13 km, two-wave multiplex (11 GHZ distance)

A construction example of the bus/star-type total digital CATV system is illustrated in Figure 3, while the main transmission elements are indicated in Table 6. The main lines for this system (the line between the center and HUB: bus, 900Mb/s M-TPC) contain an 8-channel video and 16 channel sound. Any two arbitrary channels can be selected by the video request signal (64Kb/s) transmitted from each subscriber, and they will be distributed to the subscribers through the subscriber network (the line between HUB and the subscriber: star, 200Mb/s M-TPC).

On the other hand, the network construction of the double star-type subscriber-based optical communications system is illustrated in Figure 4, while the main elements are indicated in Table 7. This system is designed based on the double star network construction, in which the optical star coupler is installed near the subscriber. To maintain reliability, the optical star coupler and the nodes are connected by several channels. Therefore, it is proposed that the outgoing circuit be transmitted at high speed while the incoming circuit be transmitted by TDM. In addition, the WDM-based overplay method is adopted for the additional new service. Since the outgoing circuit is of the broadcasting type under the bus/star or double star type network construction, attempts must be made to code the E-E service from the standpoint of maintaining its privacy. Furthermore, it is very important to establish a low-cost high-speed optical transmission technology (Gb/s) to carry out video distribution more effectively.

To comply with the demand for large volume and various kinds of service expected in the future, a proposal has reportedly been made regarding the subscriber network called "L-ITN." Figure 5 shows the network construction of L-ITN. This system comprises optical fiber with a multi-lane ring construction and a TPN node, which can transmit information from the subscribers to different lanes depending on the service characteristics. This system calls for the installation of a transmission channel ranging form 1Gb/s for the subscriber lines and one from 10Gb/s between the TPN nodes, so that the network can comply with the various transmission speeds, qualities, and connection modes.

Another proposal has reportedly been made regarding the subscriber-based optical communications system which uses coherent transmission technology. Coherent transmission technology applying to the key systems has been studied since it would offer excellent sensitivity to the receiving system. Specific attention has been placed on the study of the submarine repeating system which requires long distance and non-repeating transmission. It is capable of building up the subscriber-based optical transmission system, which is rich in both flexibility and expandability, with the application of the frequency division multiplex (FDM), which indicates the other feature of coherent transmission technology. Figure 6 illustrates a construction example of the subscriber-based optical communication system in which the optical FDM has been adopted. In this case, the two wavelength transmission experiment, i.e., an experiment involving a wavelength of 450Mb/s and

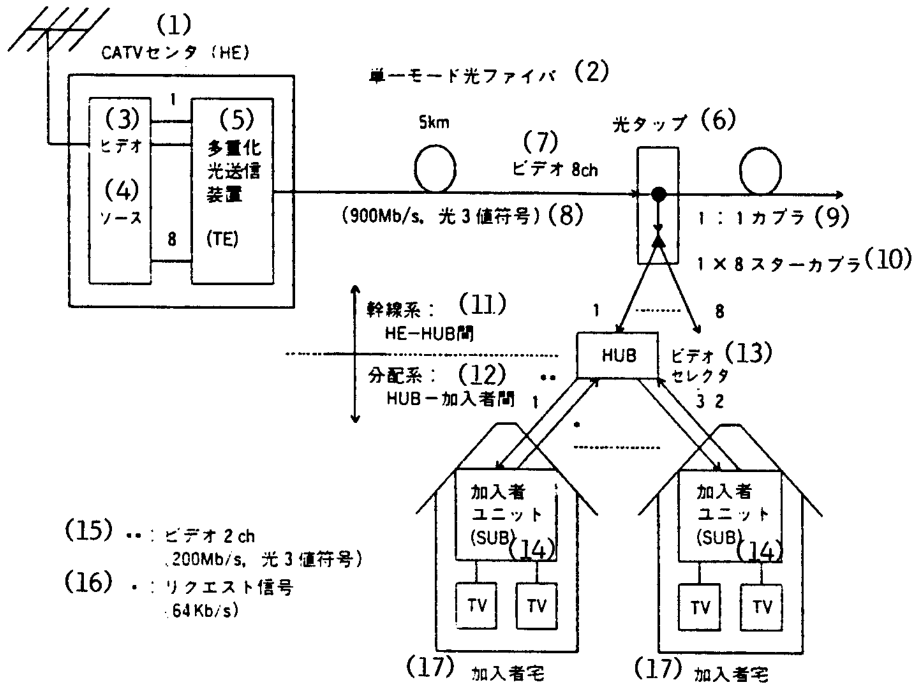

Figure 3. Basic Construction of Bus/Star-Type Digital Optical CATV System

Key:

1. CATV Center (HE)
2. Single mode optical fiber
3. Video
4. Source
5. Multiplex optical transmission equipment (TE)
6. Optical tap
7. Video 8 ch
8. (900 Mb/s, optical three-valued signal)
9. 1 : 1 coupler
10. 1 x 8 star coupler
11. Trunk line system: between HE-HUB
12. Distribution system: between subscriber-HUB
13. Video selector
14. Subscriber's unit (SUB)
15. **: Video 2 ch
    (200 Mb/s, optical three valued signal)
16. * : Request signal
    (64 Kb/s)
17. Subscriber's home

Table 6. Transmission Elements for Bus/Star Type Digital Optical CATV System

Item	Elements
Transmission Capacity	8 ch image + 16 ch sound
Transmission Speed	794.4 Mb/s
Transmission Line Signal	M-TPC (class 3)
Application Distance	25 km and over (single-mode optical fiber)
SNR	image: 50 dB, overtone: 80 dB and over
Non-Linear Distortion	image: DG 5 percent, DP 3 degrees

Table 7. Main Elements for Double Star-Type Wideband Subscriber-Based Network

Item	Contents
Service	Image, sound, 64 Kb/s system, future: Hn to be supplied, too
Cost	Lower than (CATV) + 64 Kb/s system)
Reliability	Double routes, multiplex node assignment (option)
Expandability	Based on WDM no installation of new line
Network Topology	Loop x star x star
Node Function	ADD/DROP multiplex, future: interchange of node area

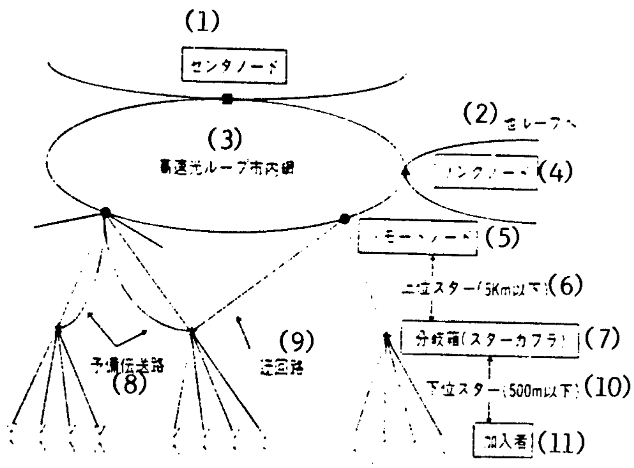

Figure 4. Basic Construction for Double Star-Type Wideband Subscriber-Based Network

Key:

1. Center node
2. To other loops
3. High speed optical loop city network
4. Link node
5. Remote node
6. Upper star (5 km and below)
7. Branch box (star coupler)
8. Stand-by transmission line
9. Alternate route
10. Lower star (500 ml and below)
11. Subscriber

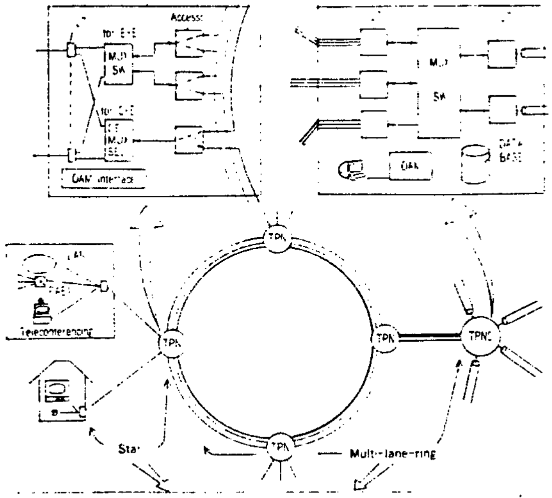

Fiber	SM (standard grade)	SM (High grade)
Distance	< 2km	< 20km
Bit rate	~ 1 Gb/s	~ 10 Gb/s
Number of fiber/TPN	~ 1000	~ 30

Figure 5. Basic Construction of Multi-Lane Ring-Type Subscriber-Based Optical Network

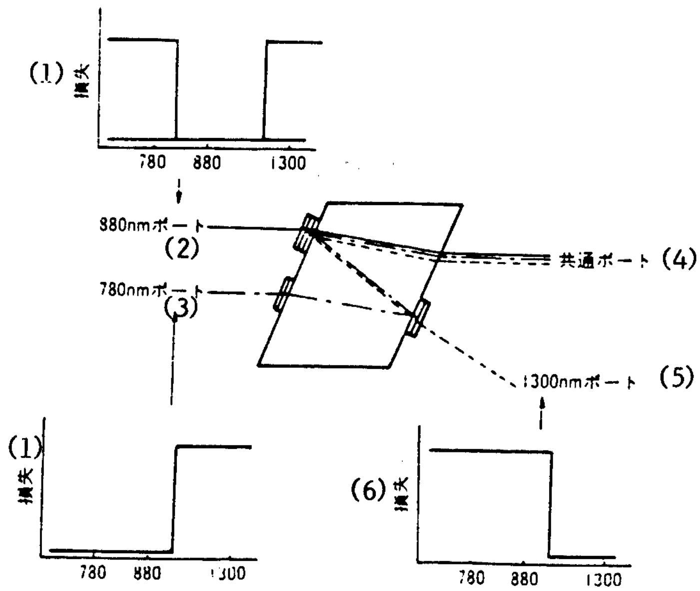

Figure 6. Construction of Optical Combining and Branching Filter Block and Filter Characteristics

Key:

1. Loss
2. 880 nm port
3. 780 nm port
4. Common port
5. 1300 nm port
6. Port

utilizing an optical frequency variable filter and single mode optical fiber of 13 km, is reported. The network is of the tristar type construction in which a star coupler is used.

Finally, the authors indicate the problems to be solved in the development of the subscriber-based optical communications systems in Figure 7.

4. Postface

The authors have outlined the current status and future trends of the subscriber-based optical communications systems in Japan. The research and development of the current subscriber-based optical communications system is targeted at CATV service on the whole, and this trend is expected to continue in the future. In addition, the future trends indicate that subscriber-based optical communications adopting a bus or double star-type network construction will be introduced to the market in an effort to improve the economic efficiency by sharing the center facilities and subscriber's line, accompanied by progress in high speed TDM technology and optical FDM technology. However, it is necessary to develop the optical communications system mentioned above with specific attention paid to the connection between the existing network and the new network, which the authors believe is a more realistic approach to the problem.

The full-scale subscriber-based optical communications system will be introduced in the future, and will include the advanced countries in the world. Many different system concepts can be adopted for the subscriber-based optical communications system, depending on the service requirements and the user/network interface requirements. Attempts to provide an individual technology per system could waste developmental efforts. Therefore, it is necessary to provide more flexible expandability involving the service trends and more improved economic efficiency before offering this optical communications system to subscribers. To comply with this, it is expected that more active efforts will be made to study the future-oriented network constructions and improved economic efficiency involving the functional expandability and terminals related to digital transmission technology or VLSI.

Developmental Trend in Optical Devices

43066518 Tokyo OPTRONICS in Japanese Nov 87 pp 95-100

[Article by Tsutomu Yoshiya and Katusyuki Imoto, Hitachi, Ltd.]

[Excerpt] 1. Preface

The optical devices used for the subscriber-based optical communications system must meet the demand for higher performance and greater reliability. In addition, they must be supplied at lower cost, which

(Market)	penetration of information equipment to home penetration of FAX, electronic mail, telecommunication confab culture popularity of HA popularity of business network popularity of OA, FA	(Administration) rate policy promotion of new medium industry promotion of telecommunications business
(Service)	commercialization of HDTV expansion of advanced utilization service for network functions expansion of CATV business activation of regional telecommunications business expansion of VAN	
(Network)	custom-made by network SDN*1 ISDB*2 B-ISDN ISDN joint corporation between satellite telecommunication and ground-optical telecommunication new system for network network control MAN optical local network variable capacity control	(Standardization) high speed wideband communications quality high speed wideband communications code user/network interface HDTV study of standard and transmission format optical component standard
(System)	economic efficiency for optical system improved reliability and controllability of system OEIC ultra-high-speed VLSI ATM*3 enhancing expert system for operation system optical wave telecommunications, optical exchange signal processing transport processing	

(*1) SDN: Software Defined Network
(*2) ISDB: Integrated Service Digital Broadcasting
(*3) ATM: Asynchronous Transfer Mode

Figure 7. Various Problems Surrounding the Development of Subscriber-Based Optical Communications System

constitutes the essential requirement. Therefore, to comply with these requirements and carry out two-way transmission (incoming and outgoing) or several channel-based transmission through an optical combining and branching filter, the technology enabling the multiplexing of various kinds of light with different wavelengths is excellent in terms of economic efficiency. Therefore, this technology is used in wide areas.

In this article, the authors introduce the current status and developmental trends of a single unit optical module, an integrated-type optical module, and a waveguide-type optical device.

2. Single Unit Optical Module

Figure 1 shows the construction of a subscriber-based optical communications system as a typical model system. This system is designed to transmit various kinds of information simultaneously with a single optical fiber. The construction comprises an optical combining and branching filter required to carry out optical wavelength multiplex transmission (WDM), and light emitting diode (LED) and laser diode (LD) modules of various wavelengths as the light source on the transmission side, with pin and photo diode (PIN-PD) and avalanche photo diode (APD) modules on the receiving side. Generally, a combination of LED and PIN-PD is used for the short sections of the subscriber-based optical communications system, while a combination of LDA and PD is used for the long section. Figure 1 shows a subscriber-based optical communications system which adopts a light source with four wavelengths. Two wavelengths, i.e., 1.2 μm and 1.3 μm, are used for the two-way image transmission service, with 0.89 μm used for one-way image transmission, and 0.89 μm and 0.81 μm used for high speed digital transmission. They are all connected to a single fiber transmission path (50/125GI) with an optical combining and branching filter. The transmission side consists of all LD modules, while the receiving side adopts Ge-APD modules or Si-APD modules, depending on the wavelength.

Figure 2 [omitted] shows a single unit optical module which has been developed for the subscriber-based optical communications system. Each optical module is connected using a FC-type optical connector. Therefore, the light emitting and receiving module and the light input/output terminals of the optical combining and branching filter use the FC-type optical connector for connection or adopt the receptacle construction which allows the FC-type optical connector to be removed easily.

To connect the optical elements for the light emitting and receiving module with the optical fiber, either the but joint method, which directly connects the optical fiber with the module, or the lens connection method, which indirectly connects the optical fiber with the module through a sphere lens or a rod lens, is adopted. Either method calls for the technological establishment of precision processing and precision positioning.

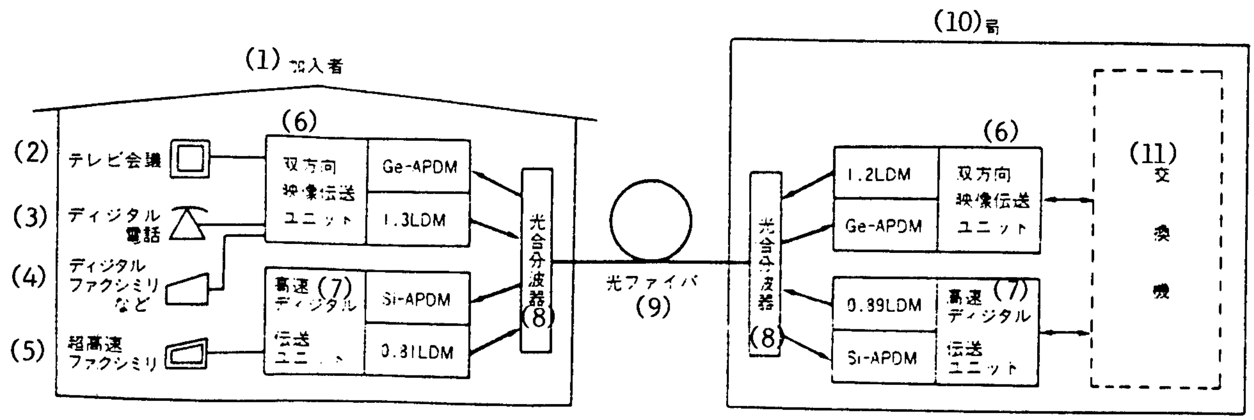

Figure 1. Example of Subscriber-Based Optical Communications System Construction

Key:
1. Subscriber
2. TV conference
3. Digital telephone
4. Digital facsimile
5. Ultra-speed facsimile
6. Two-way image transmission unit
7. High speed digital transmission unit
8. Optical combining and branching filter
9. Optical fiber
10. Station
11. Exchange

Figure 3 shows the exterior of a light combining and branching filter for four-wavelength multiplex transmission. Its main optical components include fiber, a rod lens, dielectric multiplex film filter, and glass block. They are accurately positioned, especially between the terminals connecting the common terminal on the right side in the center and the respective light emitting and receiving module, so as to minimize the coupling loss. The characteristics of the combining and branching filter vary with the system transmission concept and the wavelength. Generally, they are required to meet the following specifications:

loss of path area:	2.5 dB and below
return loss:	28 dB and over
return loss in rejection area:	26 dB and over

The single unit modules illustrated in Figure 2 [omitted] are quite advantageous in that they can be handled with ease and maintained with less care. On the other hand, they are disadvantageous in that they include a number of parts which hinder the efforts to reduce both size and cost and involve a number of portions to be precisely positioned, making it difficult to attain mass production. As a result, many attempts have been made to develop an integrated module which would allow excellent mass productivity.

3. Integrated Optical Module

The development of an integrated optical module is directed toward reducing the size and cost. Various efforts have been made to develop such an integrated optical module with specific attention paid to the following points:

(1) Install all components, such as a light emitting section, a light receiving section and an optical combining and branching filter, on the dual-inline (DIL)-type ceramic substrate for integration.

(2) Place the light emitting section and the light receiving section into a collimator package in which the optical semiconductors are integrated with the lens.

(3) Select the same configuration and dimensions for the outside construction of the collimator and use the outside shape as a reference face while assembling the ceramic substrate.

(4) Install the collimator and the light combining and branching filter to the DIL-type ceramic substrate without control based on the specified jig standard.

Figure 4 shows the basic construction of an integrated optical module with multiplex wavelength (for a short section). The service wavelength consists of three waves, i.e., 0.78 μm, 0.88 μm, and 1.3 μm according to

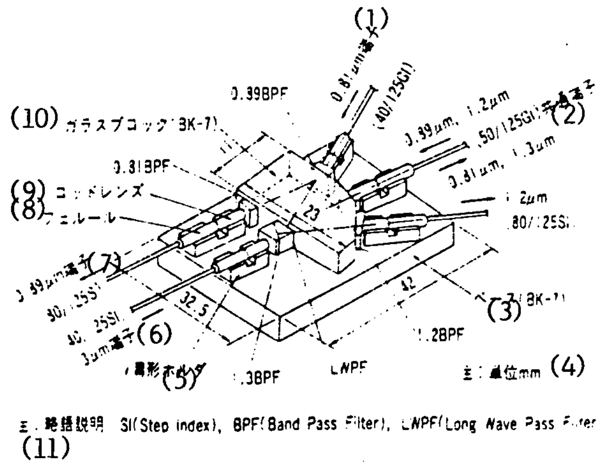

Figure 3. Construction of Optical Combining and Branching Filter

Key:

1. 0.81 µm terminal
2. (50/125 GI) common terminal
3. Base (BK-7)
4. Note: Unit mm
5. V-slot holder
6. 1.3 µm terminal
7. 0.89 µm terminal
8. Ferrule
9. Rod lens
10. Glass block (BK-7)
11. Note: acronym expansion

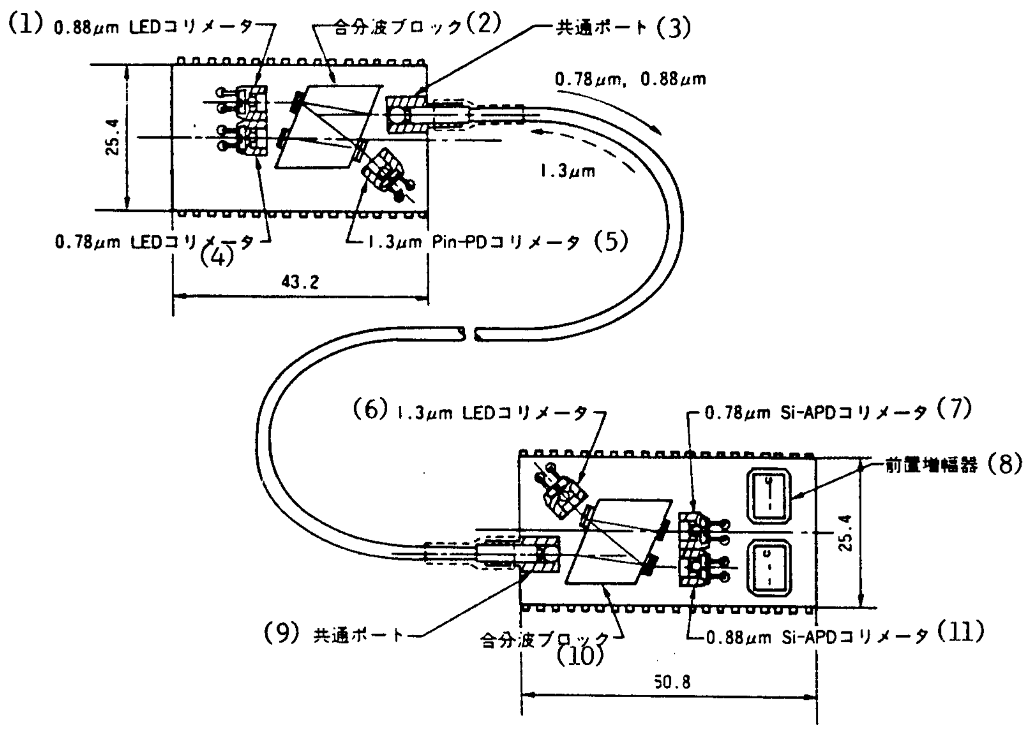

Figure 4. Construction of Wavelength Multiplex and Integrated-Type Optical Module

Key:

1. 0.88 μm LED collimator
2. Optical combining and branching filter
3. Common port
4. 0.78 μm LED collimator
5. 1.3 μm Pin-PD collimator
6. 1.3 μm LED collimator
7. 0.78 μm Si-APD collimator
8. Front amplifier
9. Common port
10. Optical combining and branching filter
11. 0.88 μm Si-APD collimator

this construction. The 0.78 μm and 0.88 μm wavelengths are used to transmit the downward signals, while the 1.3 μm wavelength is used to transmit the upward signals. The optical semiconductor element is adopted as an LED for short distance transmission in all cases. The receiving section adopts Si-APD for short wavelength, while it uses PIN-PD for long wavelengths.

Figure 5 shows the construction of an optical element collimator and an optical fiber collimator. The spherical lens used for the collimator is 3 mm in diameter on the optical element side, while a 2.5 mm diameter glass spherical lens is adopted on the optical fiber side, with specific attention paid to the overall efficiency and mass production.

The LED collimator is capable of collimating the LED-emitted light to a parallel beam which assumes the central axis of the collimator as its optical axis by applying the 3 mm diameter spherical lens, while the PD-APD collimator is capable of converging the injected parallel beam on the light receiving surface, allowing the optical axis to form the central axis of the collimator. When the collimator is assembled, the stem where the optical elements are installed must be positioned in such a manner that the optical axis can be aligned with the central axis of the collimator. After that, the stem and the collimator are fixed by laser welding and are air sealed.

The optical fiber collimator comprises an optical fiber, ferrule, spherical lens, and a non-reflecting coated glass sheet to prevent reflection.

The optical combining and branching filter is designed so that the dielectric multiplex filter is laid out with the parallel surface held in the middle. The filters, comprising a combination of a long wavelength and long path area filter and a short wavelength and short path area filter, are used to reduce the spectral limitation loss. Figure 6 shows the construction of the optical combining and branching filter and the filter characteristics.

When assembling the integrated optical module, a non-control assembling method is adopted in which a high precision assembling jig must be provided to set the optical collimator, the optical fiber collimator, and the optical combining and branching filter block into the specified positions. The components must be installed on the jig based on the external configuration standard and fixed to the ceramic substrate, properly maintaining the specified dimensional relationships. A heat-resisting adhesive agent is used to fix the components of the optical combining and branching filter, while the collimator is fixed with PbSn eutectic solder in an effort to stabilize the connections.

Table 1 shows the main elements of the integrated optical modules assembled without control. Figure 7 (omitted) shows the exterior of the module. A plug-in-type optical connector is adopted on the intra-office

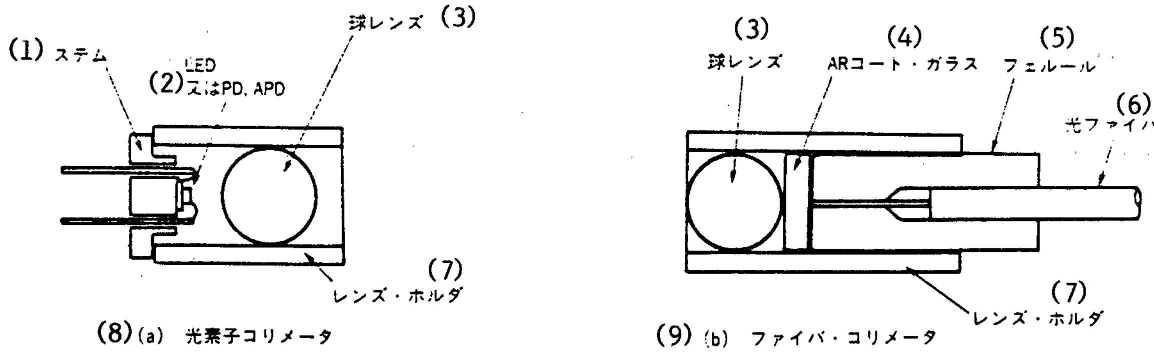

Figure 5. Optical Element Collimator and Fiber Collimator

Key:

1. Stem
2. LED or PD, APD
3. Sphere lens
4. AR coated glass
5. Ferrule
6. Optical fiber
7. Lens holder
8. (a) Optical element collimator
9. (b) Fiber collimator

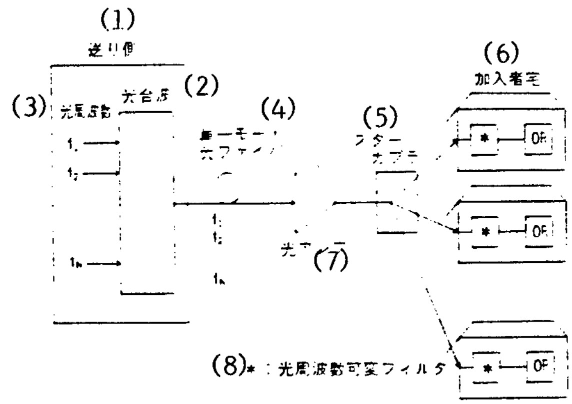

Figure 6. Basic Construction of Coherent Optical FDM Distribution-Type Subscriber-Based Communications System

Key:

1. Sender side
2. Optical combining wave
3. Optical frequency
4. Single mode optical fiber
5. Star coupler
6. Subscriber's home
7. Optical amplifier
8. *: Optical frequency variable filter

Table 1. Main Elements for Integrated-Type Optical Module

Item	Unit	Characteristic Value		
		780 nm	880 nm	1300 nm
1. Optical output	dBm	-17.2	-17.6	-25.8
2. Light receiving sensitivity	A/W	0.18	0.18	0.33
3. Cross talk attenuation	dB	37 and over		

module side, while an SC-type optical connector is adopted on the subscriber's module side for the module's pig-tail output terminal, replacing the traditional threaded FC-type optical connector. Each optical connector's fiber's end face is polished on the spherical surface, making it possible to connect with further loss reduction and higher reflecting attenuation.

The integrated optical module makes it possible to mount not only optical components, but also electric circuit components simultaneously. In this article, the authors have introduced the optical module with LED construction. The serviceability of even LD-based optical modules have already been confirmed.

4. Trends of Waveguide-Type Optical Device

4.1 Introduction

The main problem to be solved before applying the subscriber-based optical device faces is how to attain a dramatic reduction in manufacturing cost. To attain this goal, it is absolutely necessary to develop a design and manufacturing technology which excel in terms of mass productivity and reliability. Recently, research involving the waveguide-type and integrated optical device has been highlighted as a means to solve this problem. Following is the authors' introduction of recent and future trends of the research involving waveguide-type optical devices considered applicable to the subscriber-based optical devices:

4.2 Current status of optical devices

Table 2 shows the recent research trends of integrated optical devices classified per materials. Optical devices with $LiNbO_3$ have been studied for many years. For example, the research and development of a high speed optical modulator, optical switches, etc., has been actively undertaken. The research and development of compound semiconductor crystal-based optical devices centers mainly on optical and electronic integrated circuits, including the integrated construction of optical elements, both for receiving and emitting, and electronic circuits. However, at the present, no attempt has yet been made to produce monolithic products, including passive devices such as optical combining and branching filters and optical star couplers. The quart glass-based waveguides have been studied, centering on optical devices based on multimode and single mode optical fibers. As a matter of fact, optical devices for single mode service, in which the transmission loss can be reduced to 0.1 dB and below while the connection loss can be reduced to 0.1 dB, are already on the market. The passive optical devices based on these waveguides, for example, the optical combining and branching filters whose wavelengths are 1.3μm and 1.55μm are used for two-way transmission service (Figure 8) and for optical frequency dividing multiplex transmission service (Figure 9). The optical branching and

Table 2. Integrated Optical Devices Classified Per Material

Material	Typical Example	Manufacturing Method	Optical Loss	Waveguide	Application Device Example
Insulation Crystal	$LiNbO_3$	heat diffusion sputter LPE	1	multimode single mode	optical modulator optical switch
Chemical Compound	GaAs-based	LPE	0.2 to 2		optical/electronic IC
Semiconductor Crystal	InP-based	MOCVD VPE	6 to 12	single mode	optical switch optical amplifier
Glass	Quartz	CVD sputter flame accumulation	0.1 to 0.5	multimode single mode	optical combining and branching filter optical branching filter and coupler optical star coupler optical module (hybrid)

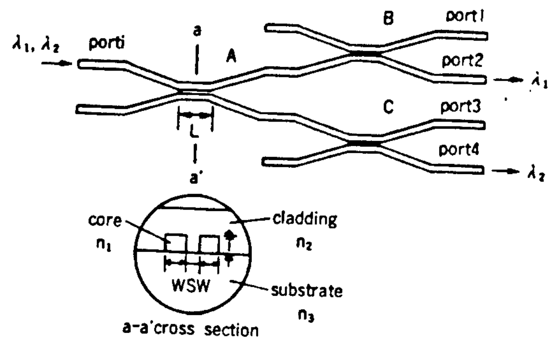

Figure 8. Optical Combining and Branching Filter for WDM Service (Directional Coupler-Type)

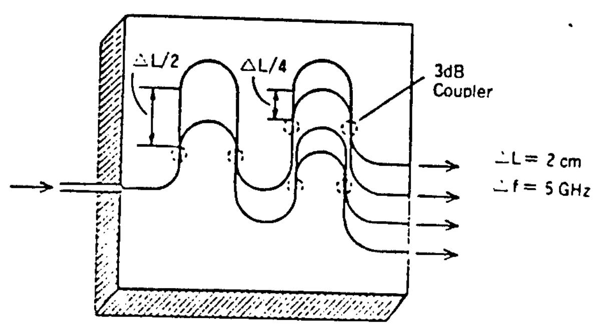

Figure 9. Optical Combining and Branching Filter for FDM Service (Mach-Zehnder Type)

coupling devices are considered promising as subscriber-based optical devices since their characteristics are found to excel in their application. In addition, recent research covers the hybrid-type optical module in which active optical elements are installed in hybrid configuration on the substrate, forming a passive optical device as illustrated in Figures 10 and 11. High expectations are placed on the research and development of this architecture.

4.3 Current status of manufacturing methods

The manufacture of $LiNbO_3$ substrate-based waveguides is already available based on the Ti diffusion and proton replacement methods and has been established from the technological standpoint as well. Compound semiconductor-based waveguides are already on the market based on the LPE method (liquid phase epitaxial development method) and MOCVD method (organic metal chemical vapor development method). However, they are subject to marked optical loss due to the characteristics of the materials. They are also highly dependent on the wavelength and suffer from azimuth during manufacture. These are very difficult problems awaiting solutions. The manufacture of quart glass-based guide wave channels are already on the market based on technologies which form glass film, such as the CVD method, the sputter method, and the flame accumulation method, as well as the patterning technology based on lithography. From the standpoint of technology, they are semiconductor applications and approach the level of practical application.

4.4 Future trends

The developmental phase of waveguide-type optical devices are expected to go through the following steps:

(1) Practical application of quart glass waveguide-type passive devices

Optical combining and branching filter, optical branching and coupling device, optical star coupler and optical filter will be available.

(2) Improved performance of hybrid-type optical module

Synthetic/quart glass waveguides will be combined with active optical elements.

The substrates of synthetic/dissimilar materials will be brought into hybrid construction.

(3) Improved performance induced by optical/electronic integrated circuits

As for the application region of these optical devices, the authors believe that applications will start in the fields which can make the best use of the features produced by the adoption of the waveguide

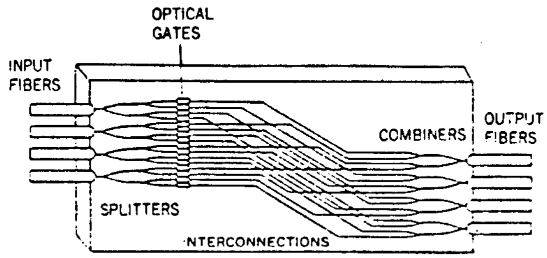

Figure 10. Optical Gate Matrix Switch

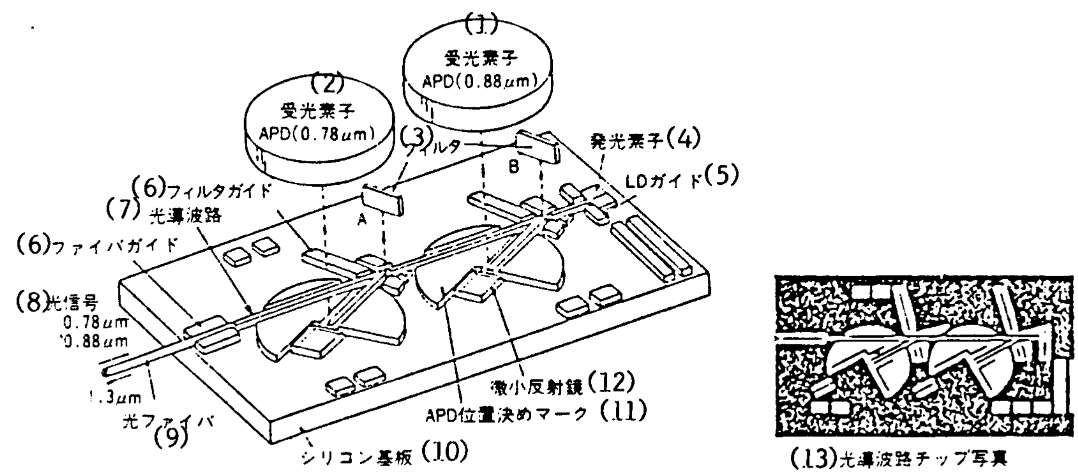

Figure 11. Wavelength Dividing Optical Combining and Branching Circuit (Multimode-Based)

Key:

1. Light receiving element APD (0.88 μm)
2. Light receiving element APD (0.78 μm)
3. Filter
4. Light emitting element
5. LD guide
6. Filter guide
7. Optical waveguide
8. Optical signal
   0.78 μm
   0.88 μm
9. 1.3 μm optical fiber
10. Silicon substrate
11. APD positioning mark
12. Minute reflecting mirror
13. Photograph of optical waveguide chip

construction for sensors or instrumentation optical circuits and expand to systems calling for high reliability, such as optical submarine relay systems, then to the subscriber-based optical communications system and coherent optical communication system.

5. Conclusion

The full-fledged introduction of the subscriber-based optical communications system is starting. To accelerate the introduction, it is absolutely necessary to digitalize all systems and make their services suitable for various purposes. The optical devices must meet the increased demand for a further reduction in size and cost in the future. Therefore, the authors believe further efforts shall be made to approach technological development, such as of OEIC [Optoelectronic Integrated Circuits].

20136/09599 - END -

10

Foreign Broadcast Information Service (FBIS) and Joint Publications Research Service (JPRS) publications contain political, economic, military, and sociological news, commentary, and other information, as well as scientific and technical data and reports. All information has been obtained from foreign radio and television broadcasts, news agency transmissions, newspapers, books, and periodicals. Items generally are processed from the first or best available source; it should not be inferred that they have been disseminated only in the medium, in the language, or to the area indicated. Items from foreign language sources are translated. Those from English-language sources are transcribed, with the original phrasing and other characteristics retained.

Headlines, editorial reports, and material enclosed in brackets [ ] are supplied by FBIS/JPRS. Processing indicators such as [Text] or [Excerpts] in the first line of each item indicate how the information was processed from the original. Unfamiliar names which are rendered phonetically or transliterated by FBIS/JPRS are enclosed in parentheses. Words or names preceded by a question mark and enclosed in parentheses were not clear from the original source but have been supplied as appropriate to the context. Other unattributed parenthetical notes within the body of an item originate with the source. Times within items are as given by the source.

SUBSCRIPTION/PROCUREMENT INFORMATION

The FBIS DAILY REPORT contains current news and information and is published Monday through Friday in 8 volumes: China, East Europe, Soviet Union, East Asia, Near East & South Asia, Africa (Sub-Sahara), Latin America, and West Europe. Supplements to the DAILY REPORTs may also be available periodically and will be distributed to regular DAILY REPORT subscribers. JPRS publications generally contain less time-sensitive information and are published periodically. Current JPRS publications are listed in *Government Reports Announcements* issued semi-monthly by the National Technical Information Service (NTIS), 5285 Port Royal Road, Springfield, Virginia 22161 and the *Monthly Catalog of U.S. Government Publications* issued by the Superintendent of Documents, U.S. Government Printing Office, Washington, D.C. 20402.

U.S. Government offices may obtain subscriptions to the DAILY REPORTs or JPRS publications (hardcovers or microfiche) at no charge through their sponsoring organizations. DOD consumers are required to submit requests through appropriate command validation channels to DIA, RTS-2C, Washington, D.C. 20301. (Telephone: (202) 373-3771, Autovon: 243-3771.) For additional information or assistance, call FBIS, (703) 527-2368, or write to P.O. Box 2604, Washington, D.C. 20013.

The public may subscribe to either hardcover or microfiche versions of the DAILY REPORTs and JPRS publications through NTIS at the above address or by calling (703) 487-4630. Subscription rates will be provided by NTIS upon request. Subscriptions are available outside the United States from NTIS or appointed foreign dealers. Back issues or single copies of the DAILY REPORTs and JPRS publications are not available. New subscribers should expect a 30-day delay in receipt of the first issue.

Both the DAILY REPORTs and the JPRS publications are on file for public reference at the Library of Congress and at many Federal Depository Libraries. Reference copies may also be seen at many public and university libraries throughout the United States.